



Late Miocene contourite depositional system of the Gulf of Cádiz: The sedimentary signature of the paleo-Mediterranean Outflow Water

Zhi Lin Ng^{a,*}, F. Javier Hernández-Molina^a, Débora Duarte^{a,b}, Cristina Roque^{c,d}, Francisco J. Sierro^e, Estefanía Llave^f, M. Amine Manar^g

^a Department of Earth Sciences, Royal Holloway University of London, Egham TW20 0EX, UK

^b Instituto Português do Mar e da Atmosfera (IPMA), 1749-077 Lisboa, Portugal

^c Estrutura de Missão para a Extensão da Plataforma Continental (EMEPC), 2770-047 Paço de Arcos, Portugal

^d Instituto Dom Luiz (IDL), Faculdade de Ciência da Universidade de Lisboa, 1749-016 Lisboa, Portugal

^e Departamento de Geología, Universidad de Salamanca, 37008 Salamanca, Spain

^f Instituto Geológico y Minero de España (IGME), 28003 Madrid, Spain

^g Office National des Hydrocarbures et des Mines (ONHYM), B.P. 99 Rabat, Morocco

ARTICLE INFO

Editor: Michele Rebesco

Keywords:

Contourite depositional system

Late Miocene

Paleo-MOW

Tectonic deformation

Gulf of Cádiz

North Atlantic

ABSTRACT

Late Miocene contourite deposits related to the paleo-Mediterranean Outflow Water (MOW) were identified in the Betic and Rifian corridors prior to the restriction of the Mediterranean-Atlantic gateway during the latest Miocene. In this study, we identified for the first time their downstream continuation in the Gulf of Cádiz through seismic stratigraphic analysis and the interpretation of contourite diagnostic features. The late Miocene contourite depositional system (CDS) consists of three stages (*initial*-, *growth*-, and *maintenance-drift*) which recorded the late Tortonian to early Messinian evolution from weak to vigorous bottom current flow in the Gulf of Cádiz prior to its cessation in the middle to late Messinian, represented by the *buried-drift* stage. Development of the CDS in the Gulf of Cádiz is coeval to a period when the continental margins were affected by regional deformation. Tectonism and diapirism, on top of sedimentary and climatic factors, exerted control on drift distribution and dimensions. However, dataset limitations hindered detailed analysis on the effect of deformation on CDS evolution. Overall, the long-term evolution of the late Miocene CDS across the Gulf of Cádiz towards the West Iberian margin suggests strengthening of paleo-MOW during the late Miocene which has significant impact on the North Atlantic ocean circulation and the late Miocene global cooling trend.

1. Introduction

Contourites provide valuable information for oceanographic and climatic changes of the past through the retainment of sedimentological, paleontological and geochemical properties related to the temporal and spatial variability in ocean circulation patterns (Rebesco et al., 2014). One of the key diagnostic criteria of a contourite depositional system (CDS) is the identification of depositional and erosional features through the interpretation of morphological features and acoustic facies using seismic reflection data (e.g., Faugères et al., 1999; Nielsen et al., 2008; Rebesco et al., 2014). However, tectonic evolution of the continental margin and the degree of deformation imposed on original deposits throughout the geological history could complicate the identification of these features, particularly for ancient contourite records. Moreover in active tectonic

settings, *syn*-tectonic deformation also play an important role in controlling the morphology and stacking pattern of contourite deposits (e.g., Reed et al., 1987; Bailey et al., 2021). It modifies the typical configuration of contourite drifts, making their identification difficult and thus still remains as one of the less studied issues in contourite research.

The Gulf of Cádiz is home to one of the best-known examples of contourite depositional systems in the world, where its Pliocene and Quaternary sedimentary succession have been studied in detail, particularly during and after the International Ocean Drilling Program (IODP) Expedition 339 (Expedition 339 Scientists, 2012; Hernández-Molina et al., 2013; Stow et al., 2013). This Pliocene-Quaternary CDS evolved along the Southwest Iberian margin as a consequence of the Mediterranean Outflow Water (MOW) exiting through the Strait of Gibraltar (or Gibraltar gateway) from the early Pliocene to the present (Hernández-

* Corresponding author.

E-mail address: Zhi.Ng.2016@live.rhul.ac.uk (Z.L. Ng).

<https://doi.org/10.1016/j.margeo.2021.106605>

Received 1 February 2021; Received in revised form 28 June 2021; Accepted 12 August 2021

Available online 15 August 2021

0025-3227/© 2021 The Authors.

Published by Elsevier B.V. This is an open access article under the CC BY-NC-ND license

(<http://creativecommons.org/licenses/by-nc-nd/4.0/>).

Molina et al., 2016). This configuration was established since the reopening of the Mediterranean-Atlantic exchange following the end of the Messinian salinity crisis (5.97–5.33 Ma; Flecker et al., 2015; Manzi et al., 2018). Prior to the middle to late Messinian restriction of the Mediterranean basin (Ng et al., 2021), the exchange of water-mass between the Mediterranean and the Atlantic took place through the Betic and Rifian corridors (or gateways) during the late Tortonian to early Messinian (Krijgsman et al., 2018). This notion was substantiated through the identification of contourite deposits bearing the signature of the paleo-MOW, in the outcrops along the corridors onshore south of Spain and north of Morocco, respectively (Martín et al., 2009; Capella et al., 2017a; de Weger et al., 2020). However, the downstream continuation of this late Miocene CDS in the Gulf of Cádiz towards the West Iberian margin has yet to be located. The ancient contourite

deposits in the onshore Betic-Rif chain, including the foreland and intramontane basins (Martín et al., 2009; Capella et al., 2017a), are only able to give a glimpse of the bigger picture of the paleo-MOW evolution through fieldwork observation of small- to medium-scale features where permitted by outcrop exposure (Rebesco et al., 2014). Whereas, unearthing the subsurface system offshore in the Gulf of Cádiz with the use of seismic reflection data will provide an opportunity for the comprehension of its wider regional implications, including insights into the evolution of the paleo-MOW circulation after its exit from the Mediterranean and its influence on the North Atlantic paleoceanography and paleoclimate during the Tortonian to Messinian stages, where it is thought to have a significant contribution to the global climate cooling of the late Miocene (Capella et al., 2019).

The criteria for the recognition of the large scale CDS features have

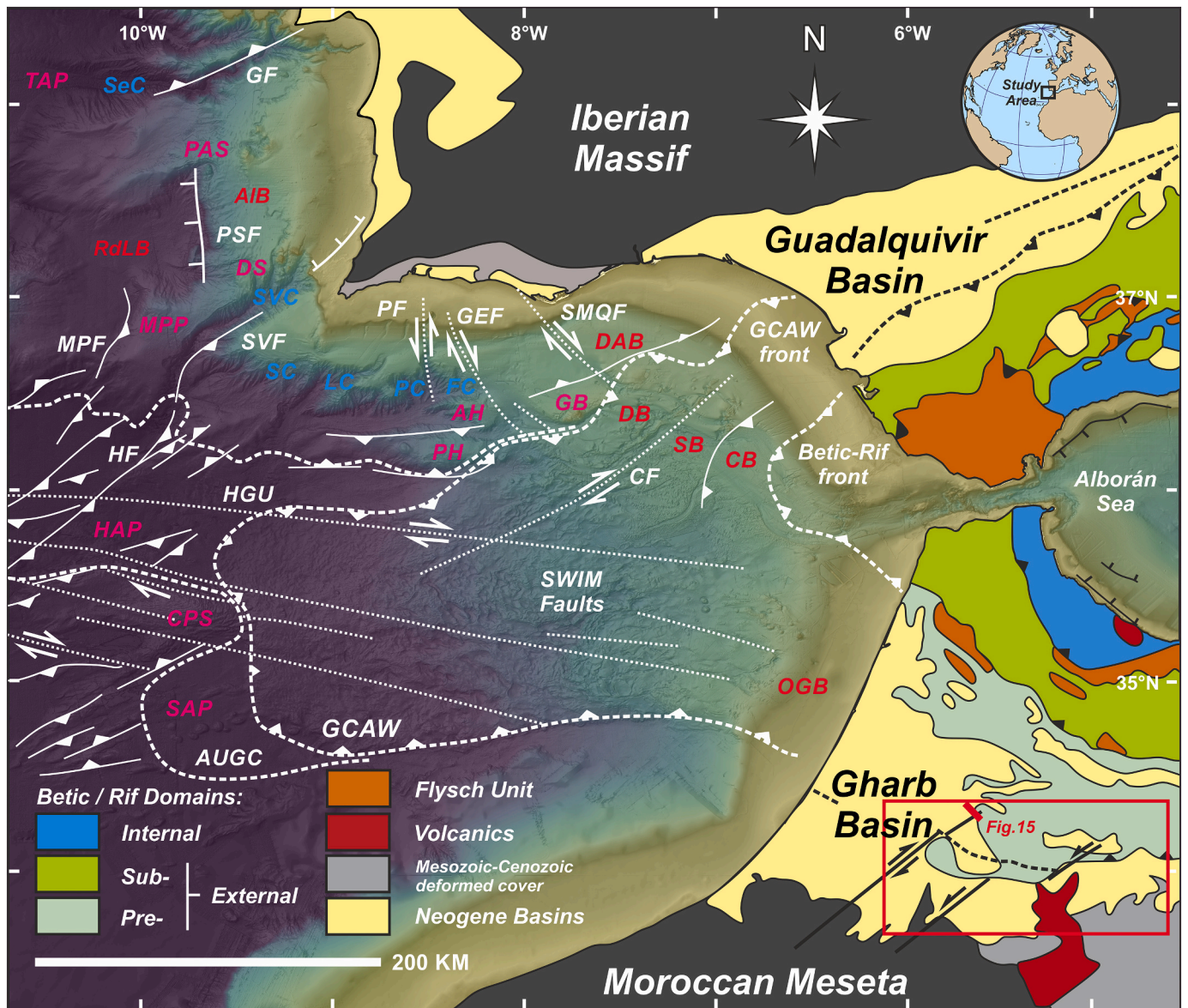


Fig. 1. Geological map showing the main structural units of the Betic-Rif orogeny (AUGC: Allochthonous unit of the Gulf of Cádiz; GCAW: Gulf of Cádiz accretionary wedge), tectonic features of the Gulf of Cádiz (AH: Albufeira high; CF: Cádiz fault; CPS: Coral Patch seamount; DS: Descobridores seamount GB: Guadalquivir bank; GEF: Gil Eanes fault; GF: Grandola fault; HAP: Horseshoe abyssal plain; HF: Horseshoe fault; HGU: Horseshoe Gravitational Unit; MPF: Marquês de Pombal fault; MPP: Marquês de Pombal plateau; PAS: Príncipe de Avis seamount; PDE: Pen Duick escarpment; PF, Portimão fault; PH: Portimão High; PSF: Pereira de Sousa fault; SAP: Seine abyssal plain; SMQF: São Marcos-Quarteira fault; SVF: São Vicente fault; TAP: Tagus abyssal plain), associated Neogene sedimentary basins (AIB: Alentejo basin; DAB: Deep Algarve basin; DB: Doñana basin; CB: Cádiz basin; OGB: Offshore Gharb basin; RdLB: Rincão do Lebre basin; SB: Sanlúcar basin) and sedimentary features (FC: Faro canyon; LC: Lagos canyon; PC: Portimão canyon; SC: Sagres canyon; SeC: Setúbal canyon; SVC: São Vicente canyon) (Adapted from Hernández-Molina et al., 2016).

been established in the literature, generally for examples within undeformed modern passive continental margins (Faugères et al., 1999; Hernández-Molina et al., 2008). However, there is a lack of guidelines for the diagnosis of ancient contourites which require paleogeographic and tectonic reconstructions (Hüneke and Stow, 2008), especially for tectonically active margins such as the Southwest Iberian margin and the Northwest Moroccan margin (Gràcia et al., 2003; Vergés and Fernández, 2012). In the Gulf of Cádiz, tectonic deformation due to the Betic-Rif orogeny have largely disturbed stratifications and modified original depositional structures, making geometric reconstruction of contourite drift bodies very difficult. Regional scale tectonic deformations are responsible for the modifications of basin shape and the connectivity among basins or sub-basins (Verdicchio and Trincardi, 2008), by creating structural highs including fault blocks, anticlines, sills and/or diapiric ridges, which has a significant impact on the bottom current circulation (Pellegrini et al., 2016; Duarte et al., 2020). With access to regional seismic reflection data integrated with borehole data in the study area, we could constrain the main tectonic evolution stages of the margin by implementing stratigraphic, structural and paleogeographic reconstructions. The main objectives of this contribution are a) to describe the characteristics and to analyse the distribution of the late Miocene CDS in the Gulf of Cádiz; b) to infer the evolution of the paleo-MOW circulation and the Mediterranean-Atlantic exchange from the characterization of the late Miocene CDS; and c) to evaluate the control factors for contourite deposition in an active continental margin. We also highlighted the implications and limitations for the interpretation of the identified late Miocene CDS.

2. Regional setting

2.1. Geological framework

The Gulf of Cádiz is located in the Atlantic side of the Mediterranean-Atlantic exchange, off the Strait of Gibraltar (Fig. 1). It is surrounded by the Southwest Iberian margin and the Northwest Moroccan margin. Tectonically, the Gulf of Cádiz lies on the eastern convergent segment of the Azores Gibraltar Fracture Zone, the plate boundary which separates the Iberian part of the Eurasian plate and the Nubian part of the African plate (Vergés and Fernández, 2012). The continental convergence between Iberia and Africa since the Late Cretaceous led to the formation of the Betic-Rif orogenic system in the middle Miocene, collectively known as the Gibraltar Arc (*sensu* Flinch, 1993), which includes, besides the Betic and Rif chain, the Alboran back-arc and the Guadalquivir and Gharb foreland basins (Vergés and Fernández, 2012). An eastward-dipping subduction and westward rollback of a remnant Tethyan oceanic lithosphere saw the westward migration of the Gibraltar Arc from the early to middle Miocene, which developed the Gulf of Cádiz accretionary wedge (GCAW; *sensu* Duarte et al., 2011) (Fig. 1). Mantle flow dynamics related to the subducted slab caused surface uplift of the Gibraltar Arc to achieve isostatic equilibrium (Duggen et al., 2003; Civiero et al., 2020). Gravitational collapse of the overthrust imbricated accretionary wedge produced radial emplacement of the chaotic allochthonous unit of the Gulf of Cádiz (AUGC; *sensu* Medialdea et al., 2004). It was emplaced westwards from the deformation front of the accretionary wedge (Fig. 1) towards the Horseshoe and Seine abyssal plains (Maldonado et al., 1999; Medialdea et al., 2004) until the late Tortonian (7–8 Ma; Gràcia et al., 2003). New wedges were successively emplaced advancing westward from the tectonic reactivation of the allochthonous unit as a result of NE-SW late Miocene thick-skinned compression (Medialdea et al., 2004), with coeval extensional collapse on the back (Maestro et al., 2003). In the Horseshoe Abyssal plain (Fig. 1), the chaotic unit is called the Horseshoe Gravitational Unit (*sensu* Iribarren et al., 2007), its tectonic and gravitational domains cannot be clearly differentiated. Overall, its gravitational-derived material is sourced from the AUGC to the east, and the surrounding basement highs (Fig. 1) such as the Gorringer bank and the Coral Patch ridge (Torelli

et al., 1997; Iribarren et al., 2007).

In the central Gulf of Cádiz, this massively chaotic allochthonous unit is interbedded within the late Miocene sedimentary infill (Lopes et al., 2006; Duarte et al., 2020). The base of the late Miocene sequence is marked either by the top of the accretionary wedge (GCAW, Duarte et al., 2020) or allochthonous unit (Medialdea et al., 2004), or by the regional basal foredeep unconformity (BFU; *sensu* Maldonado et al., 1999). The top of the chaotic allochthonous unit is highly irregular due to post-emplacement mobilization of sediments by salt and shale tectonism, which forms the abundant diapiric ridges in the Gulf of Cádiz (Medialdea et al., 2009). The Gulf of Cádiz Neogene basins, including the Deep Algarve, Doñana, Sanlúcar, Cádiz and the Offshore Gharb basins (Fig. 1), are bounded or separated by these diapiric ridges or structural highs, which are formed by Neogene to recent halokinesis and half grabens of Mesozoic origin respectively (Ramos et al., 2017; Duarte et al., 2020). Both the Deep Algarve and Alentejo basins (in the southern West Iberian margin, Fig. 1) initially formed during the Mesozoic rifting related to the opening of the Tethys and North Atlantic respectively (Srivastava et al., 1990; Pereira and Alves, 2013; Pereira et al., 2016; Terrinha et al., 2019a), and were since subjected to two major inversion tectonic phases linked to the Pyrenean and Betic-Rif orogenies, in the Paleogene and Miocene respectively (Terrinha et al., 2019b). The reactivation and inversion of older rift faults during the middle to late Miocene Betic paroxysm caused uplifting of the basement highs in the southern West Iberian margin (Fig. 1) (Torelli et al., 1997; Tortella et al., 1997; Zitellini et al., 2004; Pereira et al., 2011). At the southwest corner of the margins off the Cape of São Vicente, deep incisions of submarine canyons, such as the Portimão and São Vicente canyons (Fig. 1), dominated the slope. These canyons are also controlled by the steep rift-inherited faults since the onset of tectonic uplift (Terrinha et al., 2009; Pereira and Alves, 2013).

2.2. Paleoceanography and bottom current influence on sedimentation

The lithospheric uplift resulting from the compressional events in the Gibraltar Arc (Duggen et al., 2003) imposed major transformation of the Mediterranean-Atlantic water mass exchange pattern. It changed from a single wide connection until the middle Miocene into several narrow and shallow Betic and Rifian corridors in the late Miocene (Capella et al., 2019). This evolution saw the importance of the outflowing intermediate water mass from the Mediterranean into the Atlantic, known as paleo-Mediterranean Outflow Water (MOW), and the formation of the Atlantic Mediterranean Water (AMW; *sensu* Rogerson et al., 2012) by mixing with ambient Atlantic water in the corridors (Martín et al., 2009; de Weger et al., 2020) and by the Guadalquivir and Gharb basins (Capella et al., 2017a; Pérez-Asensio et al., 2012). Continuous uplifting of the Betic and Rif corridors raised the flow velocity of the paleo-MOW, and as a consequence sandy contourites were deposited (Capella et al., 2019) and eventually closed the Mediterranean-Atlantic exchange, leading to the restriction of paleo-MOW. Subsequently, Messinian salinity crisis evaporites were deposited in the Mediterranean, simultaneous to widespread deposition of hemipelagites in the Gulf of Cádiz (Flecker et al., 2015; Ng et al., 2021). The Guadalquivir and Gharb basins were thus reduced to marine embayment areas with the closure of the late Miocene gateways towards the east (Martín et al., 2009; Ivanovic et al., 2013). Following the reopening of the Mediterranean-Atlantic exchange through the Strait of Gibraltar, the Pliocene to Quaternary sedimentary evolution of the Gulf of Cádiz was dominated by bottom current circulation of the MOW and distribution of the resulting Pliocene-Quaternary contourite depositional system (CDS) along the Southwest Iberian margin (Hernández-Molina et al., 2016), the southern West Iberian margin (Rodrigues et al., 2020) and towards the North Iberian margin in the southern Bay of Biscay (Liu et al., 2020). The onset of the weak MOW since the end of the Messinian salinity crisis produced a regional unconformity across the Gulf of Cádiz and the West Iberian margin (van der Schee et al., 2016; Ng et al., 2021). The Miocene

Pliocene boundary (MPB, 5.33 Ma; *sensu* Hernández-Molina et al., 2016) separates the Miocene sediments from the Pliocene-Quaternary CDS.

The Pliocene-Quaternary CDS has been studied in detail for the Southwest Iberian margin (Llave et al., 2011; Roque et al., 2012; Hernández-Molina et al., 2016) and southern West Iberian margin (Rodrigues et al., 2020). The evolution of the Gulf of Cádiz CDS in the Southwest Iberian margin was primarily influenced by tectonics, eustasy and climate, at varying temporal scales, and can be summarised into three stages: an *initial-drift* stage with weak MOW and large sheeted or mixed drift during the early Pliocene (5.33–3.2 Ma); a *transitional-drift* stage with MOW intensification, upslope migration and moat development from late Pliocene to early Quaternary (3.2–2 Ma); and a *growth-drift* stage involving further MOW strengthening with elongated mounded or sandy sheeted drifts from late Quaternary to the present (<2 Ma), separated by major hiatuses (Hernández-Molina et al., 2016). Furthermore, the relationship between sedimentary deposition and tectonic activity is reflected in the overlapping distribution of the morphosedimentary (Hernández-Molina et al., 2003) and tectonosedimentary domains (Duarte et al., 2020). Tectonic structures such as diapiric ridges and basement highs separated the Neogene basins in the Gulf of Cádiz and split up the MOW pathways into two main cores: a warmer and less saline upper core (MU: 500–800 m; 13–14 °C and 35.7–37‰); and a colder and more saline lower core (ML: 800–1400 m; 10.5–11.5 °C and

36.5–37.5‰) (Ambar and Howe, 1979; Llave et al., 2007; García et al., 2009). The latter further splits into three branches: intermediate, principal, and southern (Louarn and Morin, 2011), as it descends across the middle slope northward, due to Coriolis deflection. Driven by density, the MOW sinks after flowing over the Camarinal Sill of the Strait of Gibraltar, mixing with the Atlantic ambient water (O'Neill-Baringer and Price, 1997; Sánchez-Leal et al., 2017) to form the AMW (Rogerson et al., 2012). It achieves neutral buoyancy as it reaches the Cape São Vicente and settles at a depth of ~1400 m above the North Atlantic Deep Water (NADW) (Hernández-Molina et al., 2016). In the southern West Iberian margin, the Sines contourite drift is deposited in the Alentejo basin coevally with the Gulf of Cadiz CDS. Yet the three-stage evolution differs slightly, starting with an *initial stage* of weak MOW and sheeted drift until the late Pliocene (5.33–2.5 Ma); followed by a *growing stage* of strengthening MOW and mounded drift from early to middle Quaternary (2.5–0.7 Ma); and ending with a *maintenance stage* from middle Pleistocene to present (<0.7 Ma), characterised by phases of MOW intensification with higher sedimentation rates, and a shift to a plastered drift stacking pattern (Rodrigues et al., 2020). At the Northwest Moroccan margin, a predominantly hemipelagic environment during the Pliocene is consistent with the absence of the MOW since the reopening of the Mediterranean-Atlantic connection through the Strait of Gibraltar. However, younger Quaternary contourite deposits with distinct

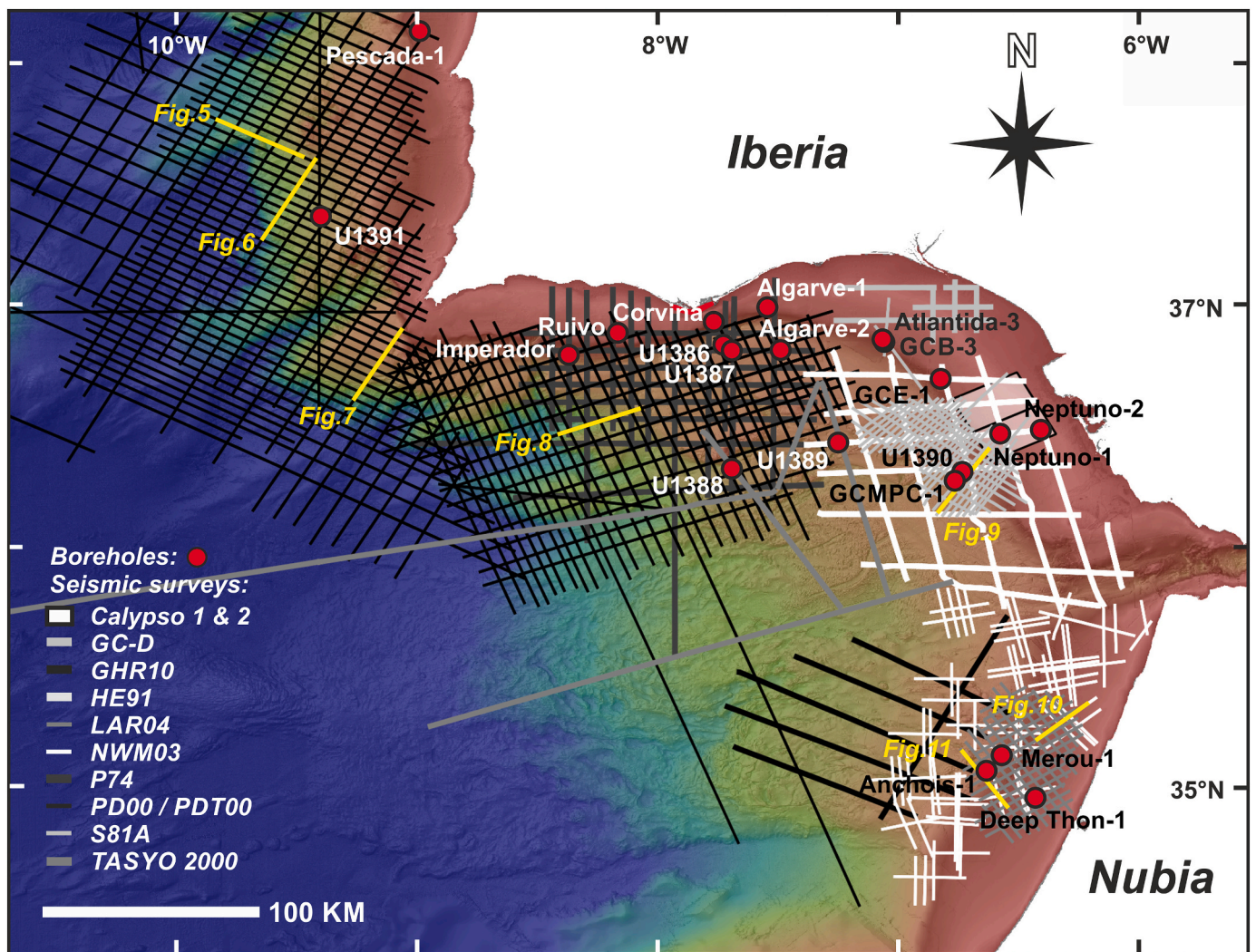


Fig. 2. Map of the dataset (including seismic surveys, boreholes, and bathymetry).

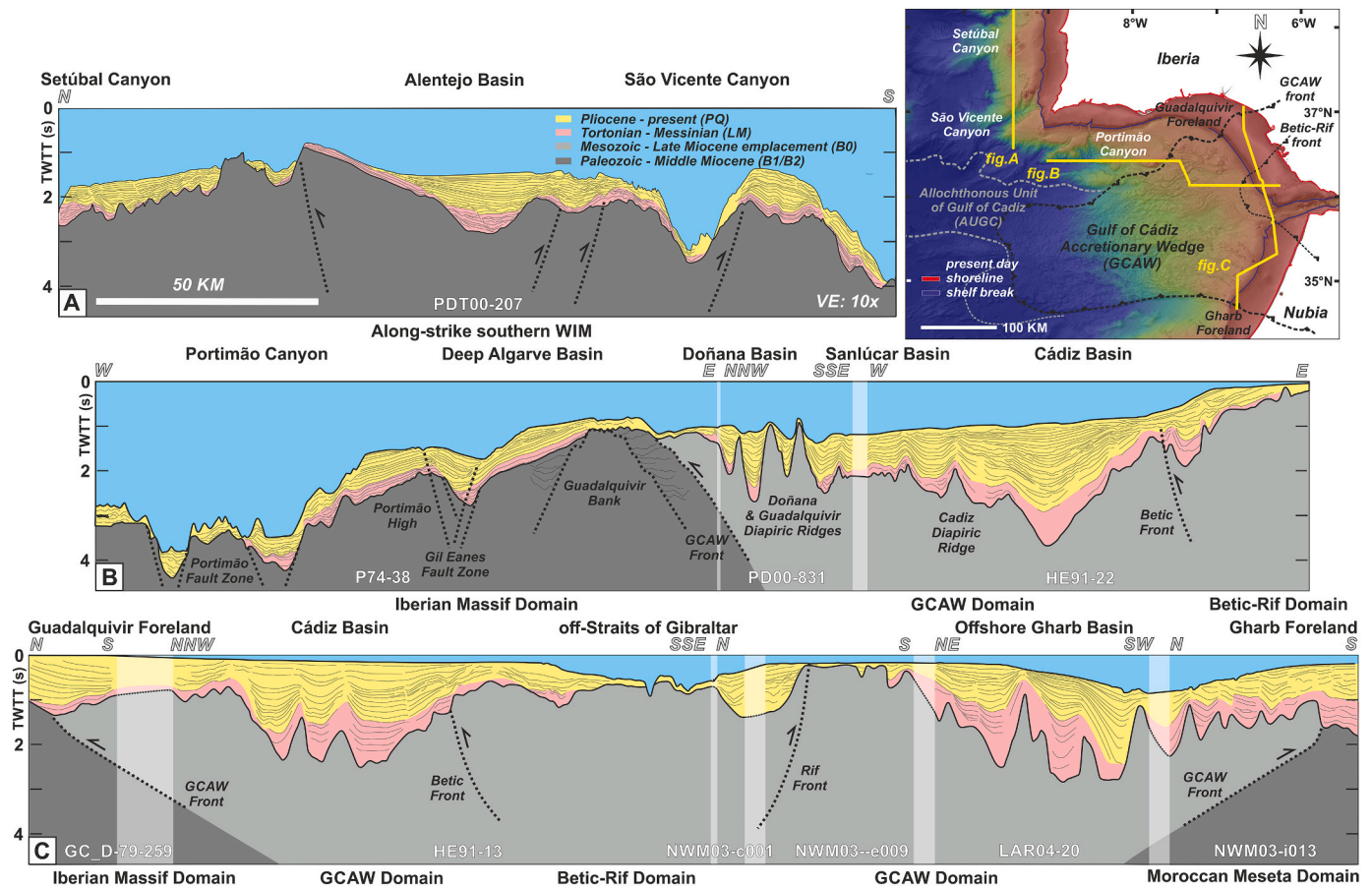


Fig. 3. Regional profiles of the study area showing the distribution of the Neogene sedimentary basins (Alentejo basin, Cádiz basin, Deep Algarve basin, Donaña basin, Offshore Gharb basin, Sanlúcar basin), tectonic domains (Betic-Rif orogeny, Gulf of Cádiz accretionary wedge, Iberian Massif, Moroccan Meseta and West Iberian passive margin) and seismic units (PQ, LM and B): a. N-S southern West Iberian margin (WIM), b. E-W Gulf of Cádiz, c. N-S Gulf of Cádiz.

evolutionary phases were identified around the Pen Duick escarpment (Fig. 1) (Vandorpe et al., 2014; Vancraeynest, 2015). These sediments were deposited under the recent influence of the Antarctic Intermediate Water (AAIW), with the absence of MOW in the southern part of the Gulf of Cádiz since the Pliocene (Vandorpe et al., 2014).

3. Methodology

3.1. Dataset

We compiled an integrated dataset of seismic reflection and borehole data from within the Gulf of Cádiz to the southern West Iberian margin (Fig. 2). The seismic data include two-dimensional (2D) multi-channel seismic reflection (MCS) profiles in time domain (TWT – two way travel time) from 8 surveys: GC-D, GHR10, HE91, LAR04, NWM03, P74, PD00, PDT00, S81A, TASYO2000 (Fig. 2); as well as 2 three-dimensional (3D) post stack time migrated (PSTM) seismic surveys, including Calypso-1 and Calypso-2, acquired from industry or academic projects and cruises predominantly with an airgun array seismic source, processed to common depth point and stack, and time migrated using standard procedures (Maldonado et al., 1999; Llave et al., 2011; Rogerson et al., 2012; Brackenridge et al., 2013; Hernández-Molina et al., 2016). Acquisition parameters for seismic surveys are available in *Supplementary Material (Table S1)*. The borehole data are from exploration wells including Algarve-2, Anchois-1, Atlantida-3, Deep Thon-1, Golfo de Cádiz B-3 (GCB-3), Golfo de Cádiz Mar Profundo C-1 (GCMPC-1), Merou-1, Neptuno-1, Neptuno-2; and the International Ocean Drilling Program Expedition 339 scientific sites (Expedition 339 Scientists, 2012;

Hernández-Molina et al., 2013; Stow et al., 2013), including U1396, U1387, U1388, U1389, U1390, and U1391 (Fig. 2).

3.2. Methods

We utilised an array of seismic attribute analyses involving signal processing and structural methods, in the order of structural smoothing with dip-guided wedge enhancement, Butterworth band-pass frequency filter (lower slope: 18 dB, 8 Hz; upper slope: 72 dB, 36 Hz), and the second derivative of the trace envelope, available at Schlumberger's Petrel E&P software platform to assist in the interpretation workflow by enhancing edges/faults and continuity of seismic events, removing noise, and identifying all reflecting interfaces within the seismic bandwidth. We then carried out the seismic stratigraphic analysis of the Gulf of Cádiz Neogene basins following Mitchum et al. (1977) in distinguishing seismo-stratigraphic units by seismic facies and boundaries, assigning geologic ages based on correlation with biostratigraphic information acquired from borehole data (summarised in Fig. 3). Afterwards, structure and isopach mapping of the major seismic discontinuities and their intervals was done to briefly reconstruct the regional paleogeography and to identify the distribution pattern of the seismic unit, respectively. The maps were generated using the Petrel E&P software with a grid increment of 50 m for both X and Y dimensions and surface operation smoothing parameters including: number of iterations – 3; filter width – 3.

The seismic interpretation was facilitated by diagnostic criteria for the recognition of contourites introduced by Faugères et al. (1999) and Nielsen et al. (2008), and the identification of depositional (drifts) and

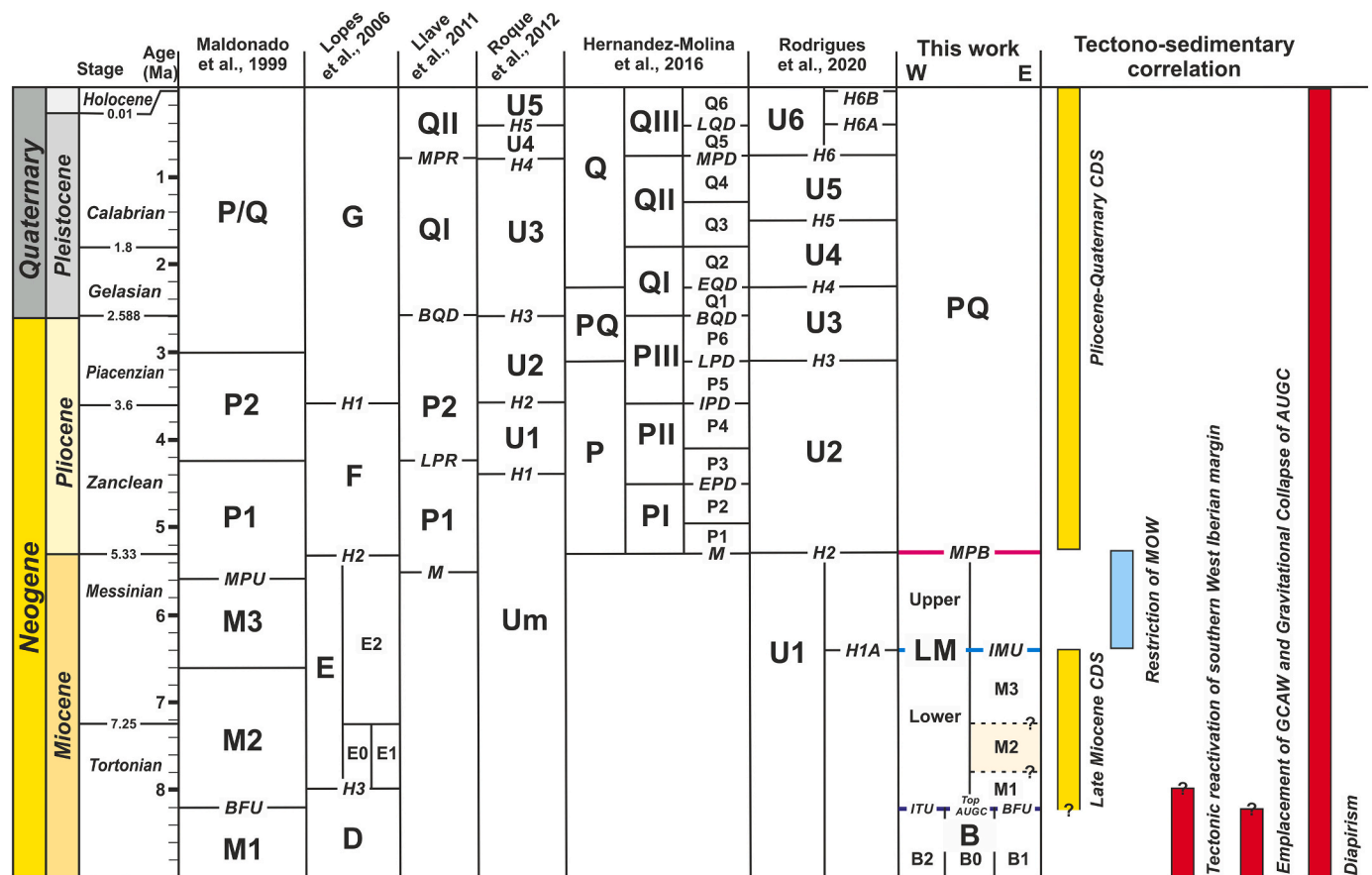


Fig. 4. Stratigraphic correlation of the main sequences (PQ, LM, B), units (Upper and Lower LM) and sub-units (M1, M2 and M3) described in the present work, including stratigraphic correlations interpreted by previous authors and main tectonic and sedimentary events in the region (Abbreviation for discontinuities, BFU: basal foredeep unconformity; IMU: intra-Messinian unconformity; ITU: intra-Tortonian unconformity; MPB: Miocene-Pliocene boundary; Top AUGC: top allochthonous unit of the Gulf of Cádiz).

erosional (channels, furrows, moats, scours) features related to bottom current action (Hernández-Molina et al., 2008; García et al., 2009; Rebesco et al., 2014). The interpreted seismic features were compared in terms of their acoustic character and distribution against other deposits of other deep-water sedimentary process, e.g., gravity flow deposits including turbidites and mass transport deposits (MTDs) (Posamentier and Erskine, 1991; Stow and Smillie, 2020), and pelagites or

hemipelagites. Interactions of multiple processes to produce mixed or hybrid deposits were taken into consideration, as reported for a modern example in the Southwest Iberian margin (Brackenridge et al., 2013; Teixeira et al., 2019; de Castro et al., 2020; Serra et al., 2020). Finally, we analysed these features to unravel the influence of the paleo-Mediterranean Outflow Water (MOW) on the sedimentary evolution of the middle slope of the Southwest Iberian, Northwest Moroccan and the

Table 1
Summary of seismostratigraphic units and boundaries of the Gulf of Cádiz and southern West Iberian margin.

Seismostratigraphic unit	Top boundary	Seismic facies and description	Depositional setting and interpretation
Pre-late Miocene	B0 (Wedge top basin) B1 (Betic foreland basin)	Top allochthonous unit of Gulf of Cádiz (AUGC) Basal foredeep unconformity (BFU)	Mega-chaotic seismic body affected by listric or thrust faulting Mesozoic to middle-late Miocene sedimentary succession and Paleozoic basement (Maldonado et al., 1999; Pereira et al., 2016)
Tortonian – Messinian	B2 (West Iberian margin) Lower LM (~8.0–~6.4 Ma) Upper LM (~6.4–5.33 Ma)	Intra-Tortonian unconformity (ITU) Intra-Messinian unconformity (IMU) Miocene Pliocene boundary (MPB)	Upper section of top-discordant high amplitude semi-continuous to chaotic reflections and lower section of homogenous chaotic reflections Upper section of high amplitude discontinuous to wavy continuous reflections and lower section of chaotic reflections See sections 4.1 and 4.2 Transparent to low amplitude continuous reflections, except for Offshore Gharb basin, which consists of intervals of high amplitude reflections in between lower amplitude intervals.
Pliocene-present	PQ (5.33–0 Ma)	Sea-floor	Late Miocene contourite depositional system (This study) Pelagites or hemipelagites, interrupted locally by turbidites (Ng et al., 2021) Pliocene-Quaternary contourite depositional system (Llave et al., 2011; Hernández-Molina et al., 2016; Roque et al., 2012)

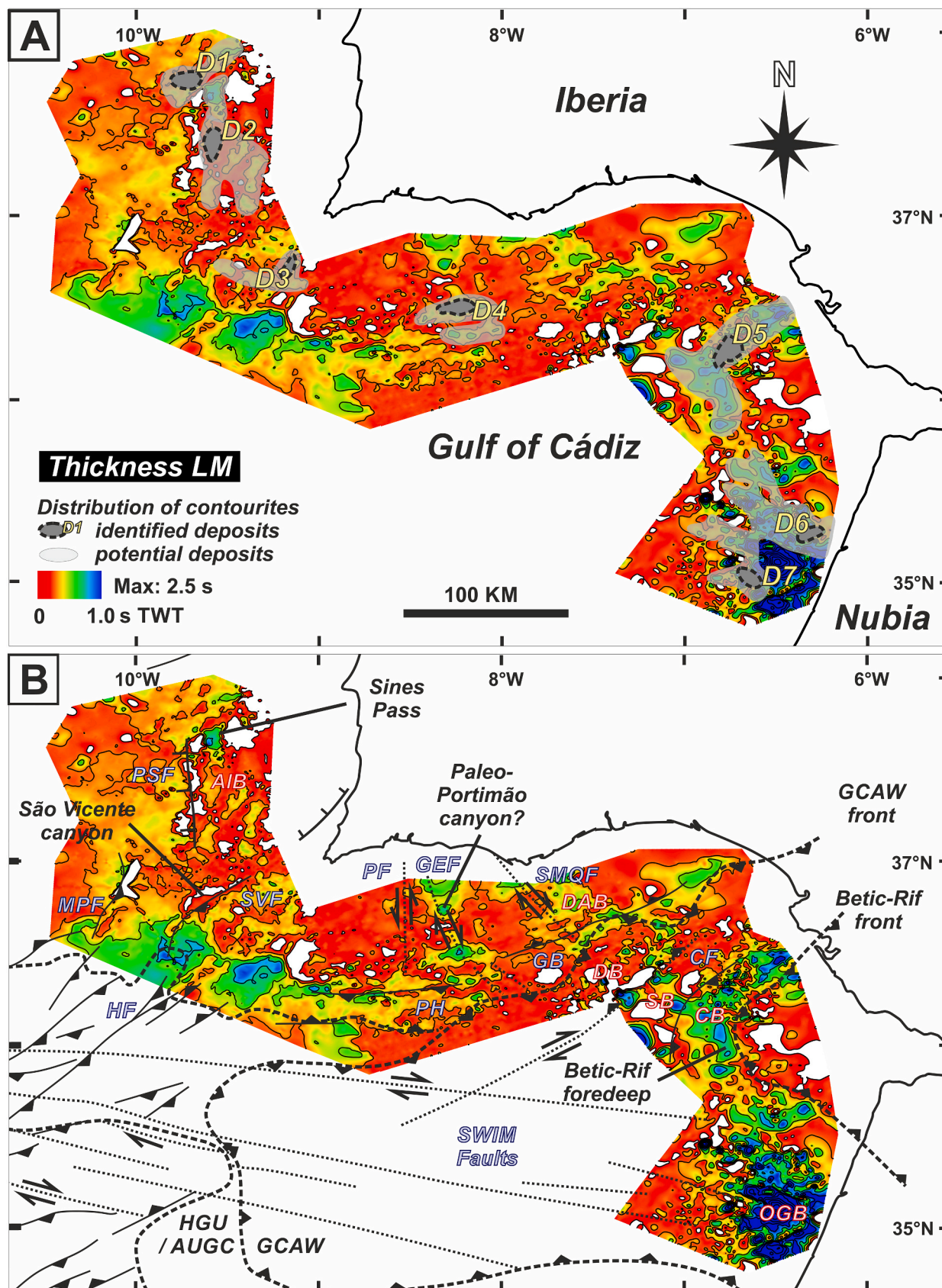


Fig. 5. Thickness map of Unit LM showing (a) the distribution of contourite deposits (D1-D7), and (b) their relationship with tectonic and sedimentary features in the Gulf of Cádiz (Structural features adapted from Hernández-Molina et al., 2016; abbreviations given in Fig. 1).

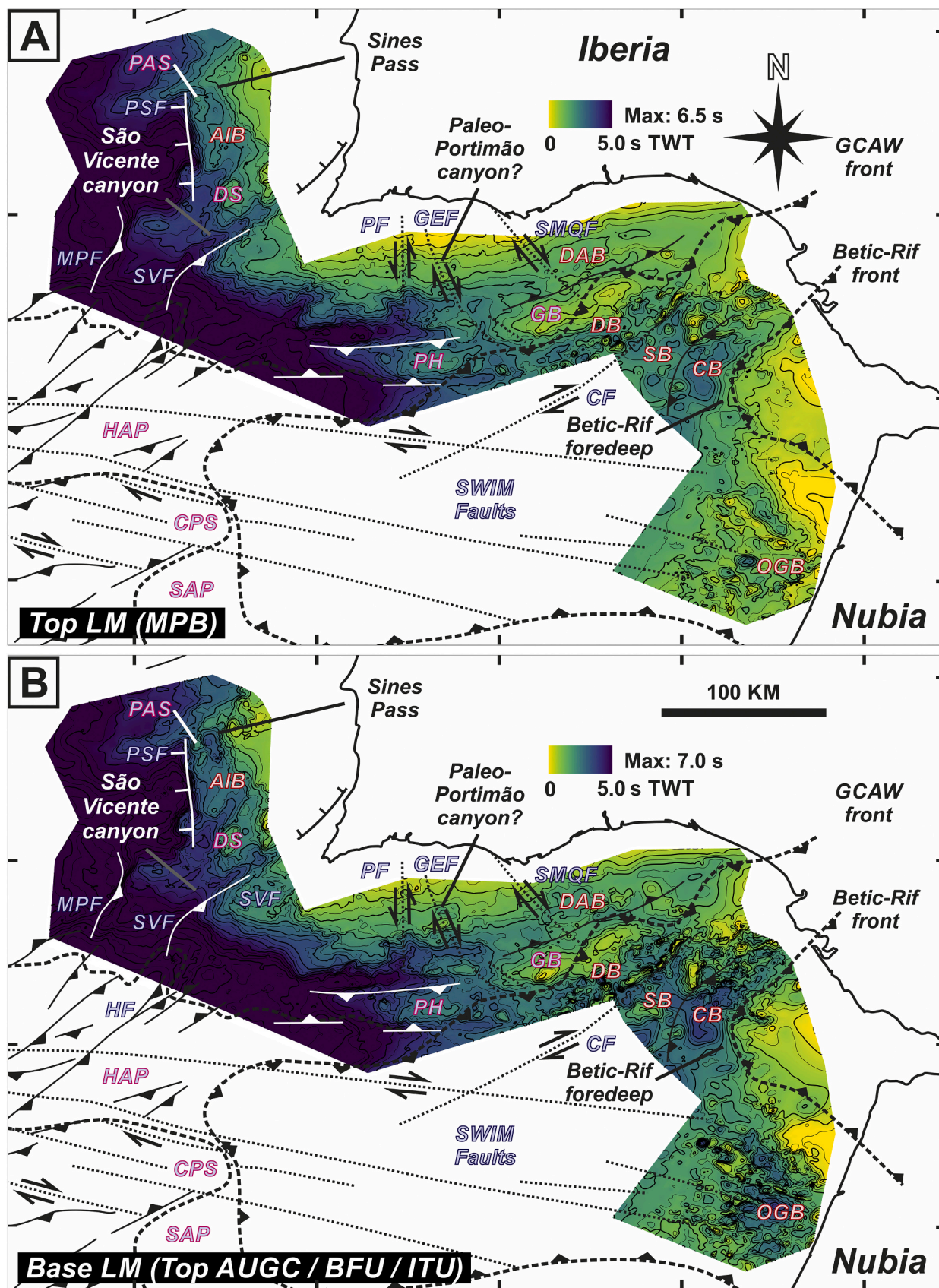


Fig. 6. Structure maps and locations of key tectonic and sedimentary features in the Gulf of Cádiz: (a) Top LM (MPB), and (b) Base LM (combination of Top AUGC, BFU and ITU) (Structural features adapted from Hernández-Molina et al., 2016; abbreviations given in Fig. 1).

southern West Iberian margins, and compare them to modern and ancient analogues in the region (Llave et al., 2001, 2007, 2011; Roque et al., 2012; Hernández-Molina et al., 2016; Teixeira et al., 2019; de Weger et al., 2020; Mencaroni et al., 2020; Rodrigues et al., 2020). We also listed the limitations and suggestions for further study in *Supplementary Material (Text S1)*.

3.3. Nomenclature

The nomenclature adopted to describe the main seismic sequences,

units, subunits, and discontinuities (Fig. 4) are adapted from previous studies (Maldonado et al., 1999; Lopes et al., 2006; Llave et al., 2011; Roque et al., 2012; Hernández-Molina et al., 2016; Rodrigues et al., 2020). They reflect the age of the intervals (e.g., PQ – Pliocene-Quaternary, LM – late Miocene). This study focuses on the late Miocene interval, previously identified as Units M2 and M1 of Maldonado et al. (1999) and Unit E of Lopes et al. (2006). The subunits (M3, M2 and M1) in this study were labelled according to their stratigraphic position from top to bottom. The Miocene-Pliocene boundary (MPB) and basal foredeep unconformity (BFU) were previously described in detail

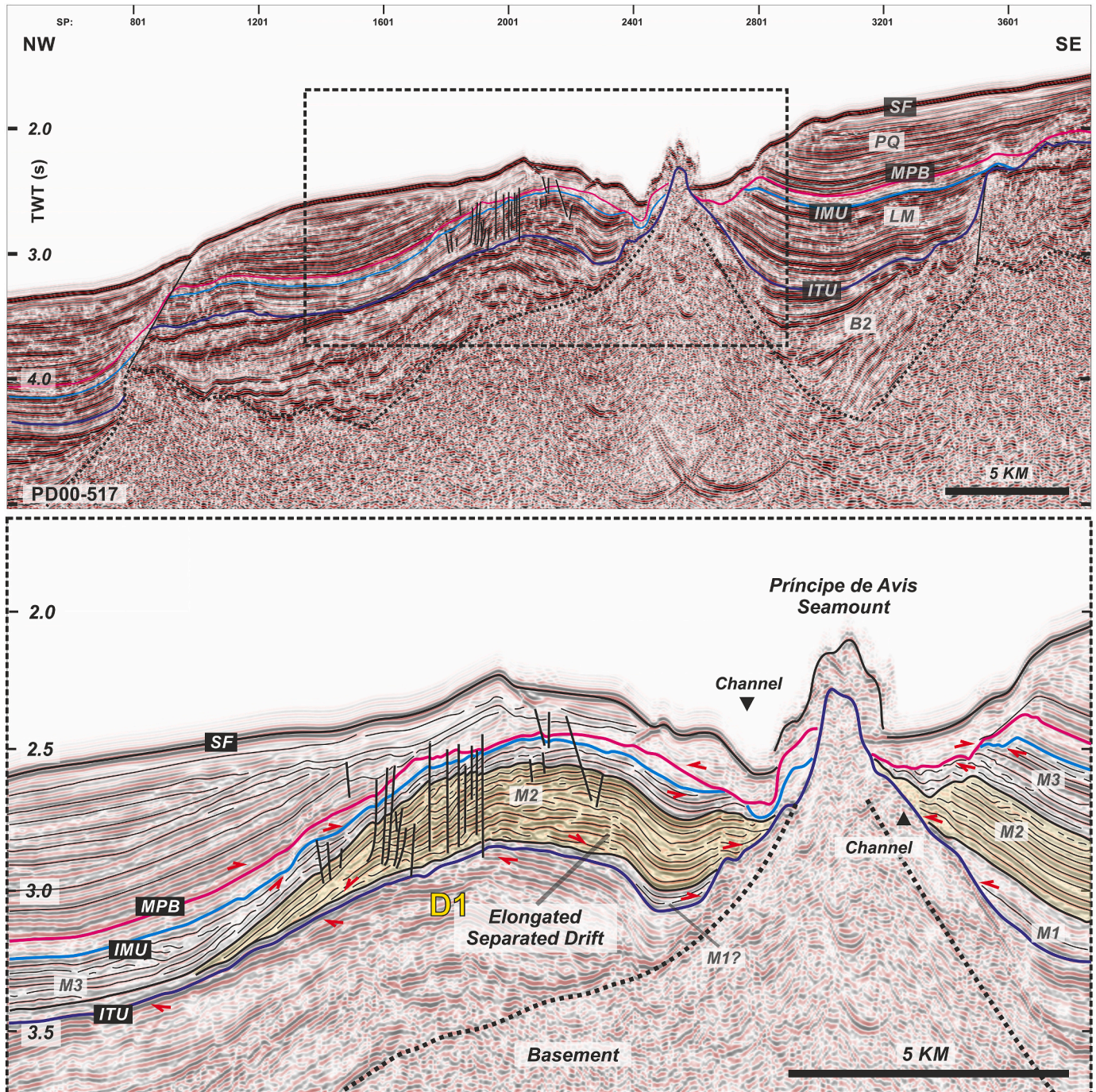


Fig. 7. Seismic profile in the middle slope of southern West Iberian margin (PD00-517) showing an elongated separated drift (D1) associated with a contourite channel west of the Príncipe de Avis seamount (PAS). Profile location given in Fig. 2. Shown are major sequences (PQ, LM and B2), subunits of Lower LM (M3 and M2) and main boundaries or discontinuities (SF: seafloor; other abbreviations given in Fig. 4; red arrows: stratal terminations). (For interpretation of the references to colour in this figure legend, the reader is referred to the web version of this article.)

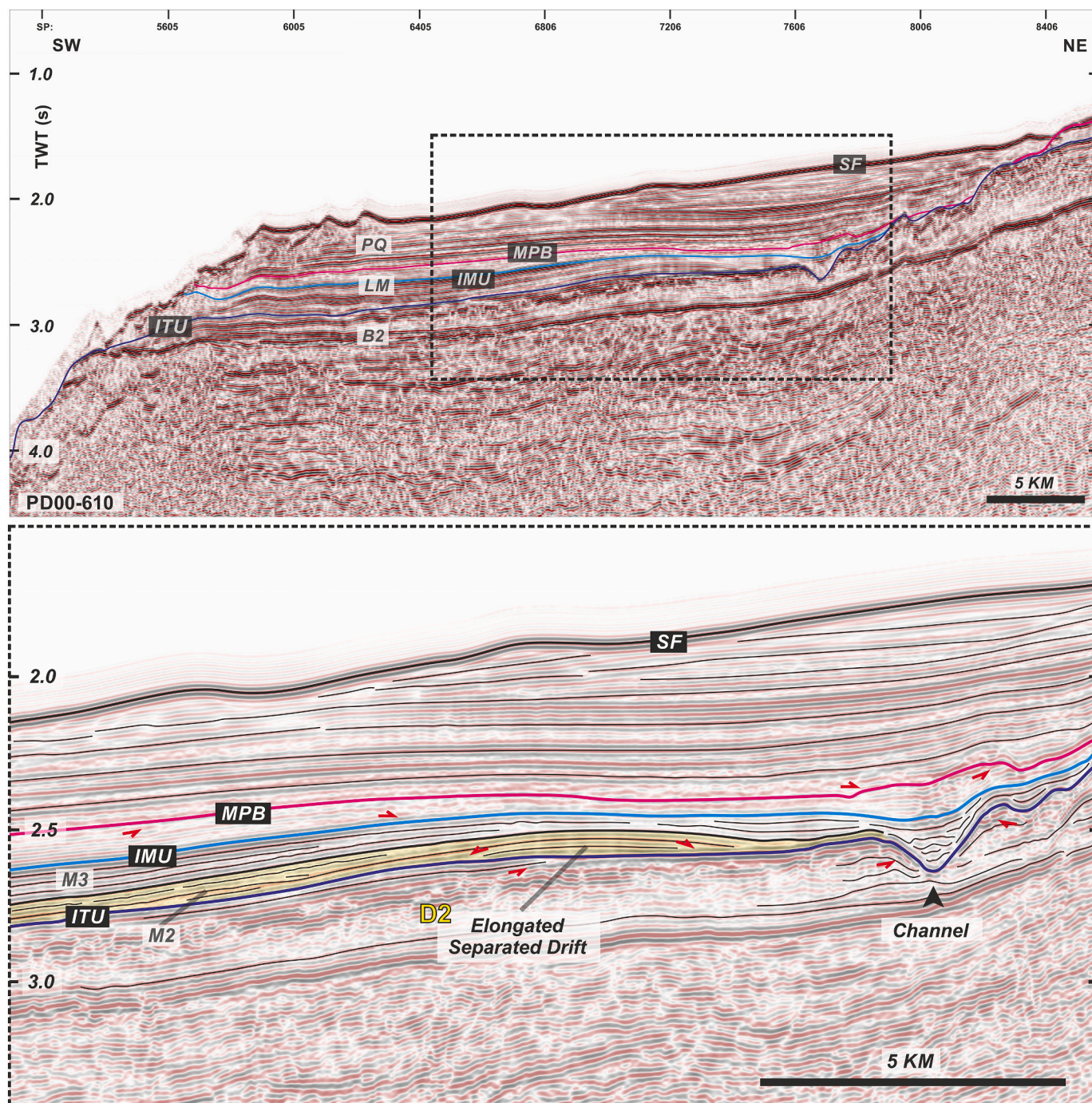


Fig. 8. Seismic profile of Alentejo basin (AlB), southern West Iberian margin (PD00–610) showing an elongated separated drift (D2) west of a contourite channel. Profile location given in Fig. 2. Major sequences (PQ, LM and B2), subunits of Lower LM (M3 and M2) and the main boundaries or discontinuities (SF: seafloor; other abbreviations given in Fig. 4; red arrows: stratal terminations). (For interpretation of the references to colour in this figure legend, the reader is referred to the web version of this article.)

by Hernández-Molina et al. (2016) and Maldonado et al. (1999) respectively, whereas the allochthonous unit of the Gulf of Cádiz (AUGC) was described by Medialdea et al. (2004). Two new discontinuities were introduced in this study (Fig. 4), namely the intra-Messinian unconformity (IMU) and the intra-Tortonian unconformity (ITU). The ITU is differentiated from the BFU due to the contrast in genetic origin of their respective margins since the Miocene (inverted passive southern West Iberian margin *versus* foreland basin of the active Southwest Iberian margin).

The term *contourites* refers to “sediments deposited or substantially reworked by the persistent action of bottom currents”, whereas *bottom currents* refers to “any persistent water current near the seafloor” (*sensu* Rebesco et al., 2014). A *contourite drift* is a “large accumulation of sediments by bottom currents”, which are classed based on their variation in location, morphologies, size, sediment patterns, construction mechanisms and controls (Faugères and Stow, 2008; Hernández-Molina et al., 2008; Rebesco et al., 2014). Whereas a *contourite depositional system* (CDS) is referred to as “the association of various drifts and related erosional

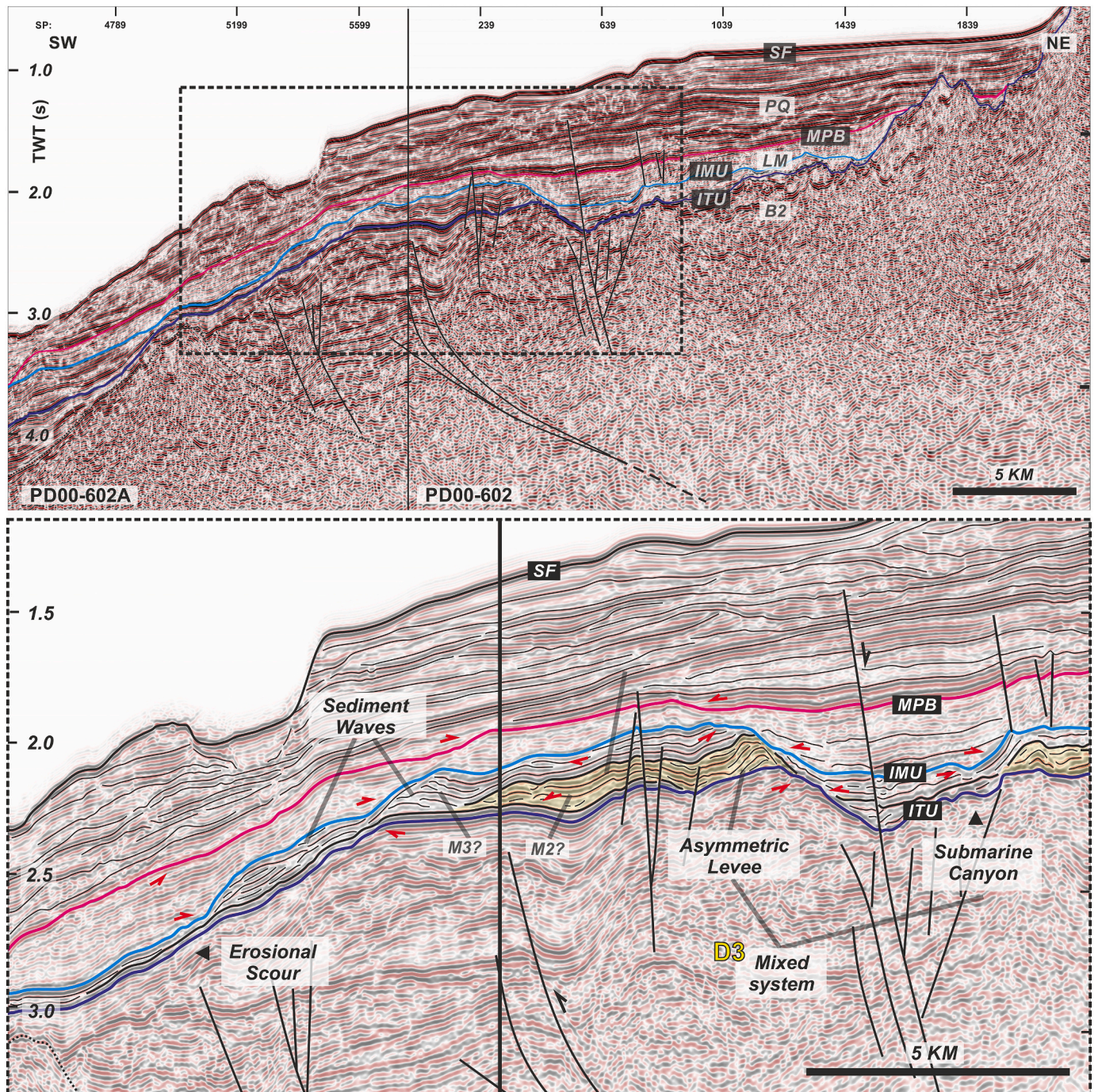


Fig. 9. Seismic profile across Sagres canyon (SC), southern West Iberian margin (PD00-602 & PD00-602A) showing an asymmetric levee and the Sagres submarine canyon associated with a mixed system (D3), as well as sediment waves and erosional scour on the middle slope. Profile location given in Fig. 2. Major sequences (PQ, LM and B2), subunits of Lower LM (M3? and M2?) and the main boundaries or discontinuities (SF: seafloor; other abbreviations given in Fig. 4; red arrows: stratal terminations). (For interpretation of the references to colour in this figure legend, the reader is referred to the web version of this article.)

features”, and could occur interbedded with other deep-water facies type, such as turbidites, pelagites and mass transport deposits (Hernández-Molina et al., 2008; Rebesco et al., 2014; de Castro et al., 2021).

4. Results

4.1. Seismic analysis: Units and boundaries

The study area is divided into three different sectors: a) the Neogene

basin of the West Iberian margin (Fig. 3a), including the Alentejo basin; b) the Betic foreland basin in the northern and northwestern Gulf of Cádiz, which includes the Deep Algarve basin (Fig. 3b); and c) the wedge top basins in the central Gulf of Cádiz, taking in the Doñana, Sanlúcar, Cádiz and Offshore Gharb basins (Fig. 3c). We identified three main regional seismic sequences from seismic analysis of all three sectors, correlated to the biostratigraphic information from the borehole (from oldest to youngest): a) Pre-late Miocene, which is distinct for three sectors (B0, B1 and B2); b) Tortonian to Messinian (LM), divided into

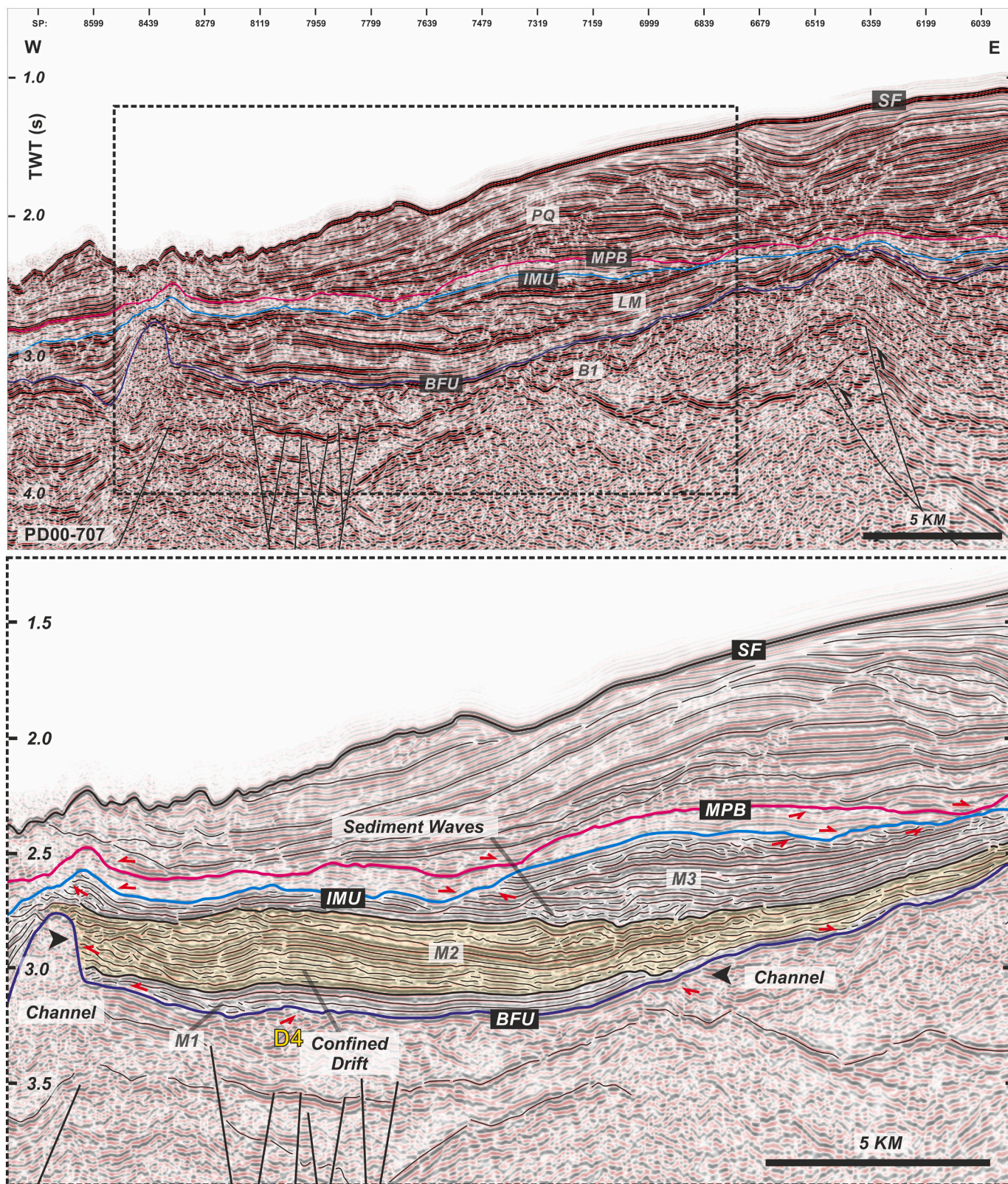


Fig. 10. Seismic profile across Faro canyon (FC), Southwest Iberian margin (PD00-707) showing a mounded confined drift (D4) and sediment waves. Profile location given in Fig. 2. Major sequences (PQ, LM and B1), subunits of Lower LM (M3, M2 and M1) and main boundaries or discontinuities (SF: seafloor; other abbreviations given in Fig. 4; red arrows: stratal terminations). (For interpretation of the references to colour in this figure legend, the reader is referred to the web version of this article.)

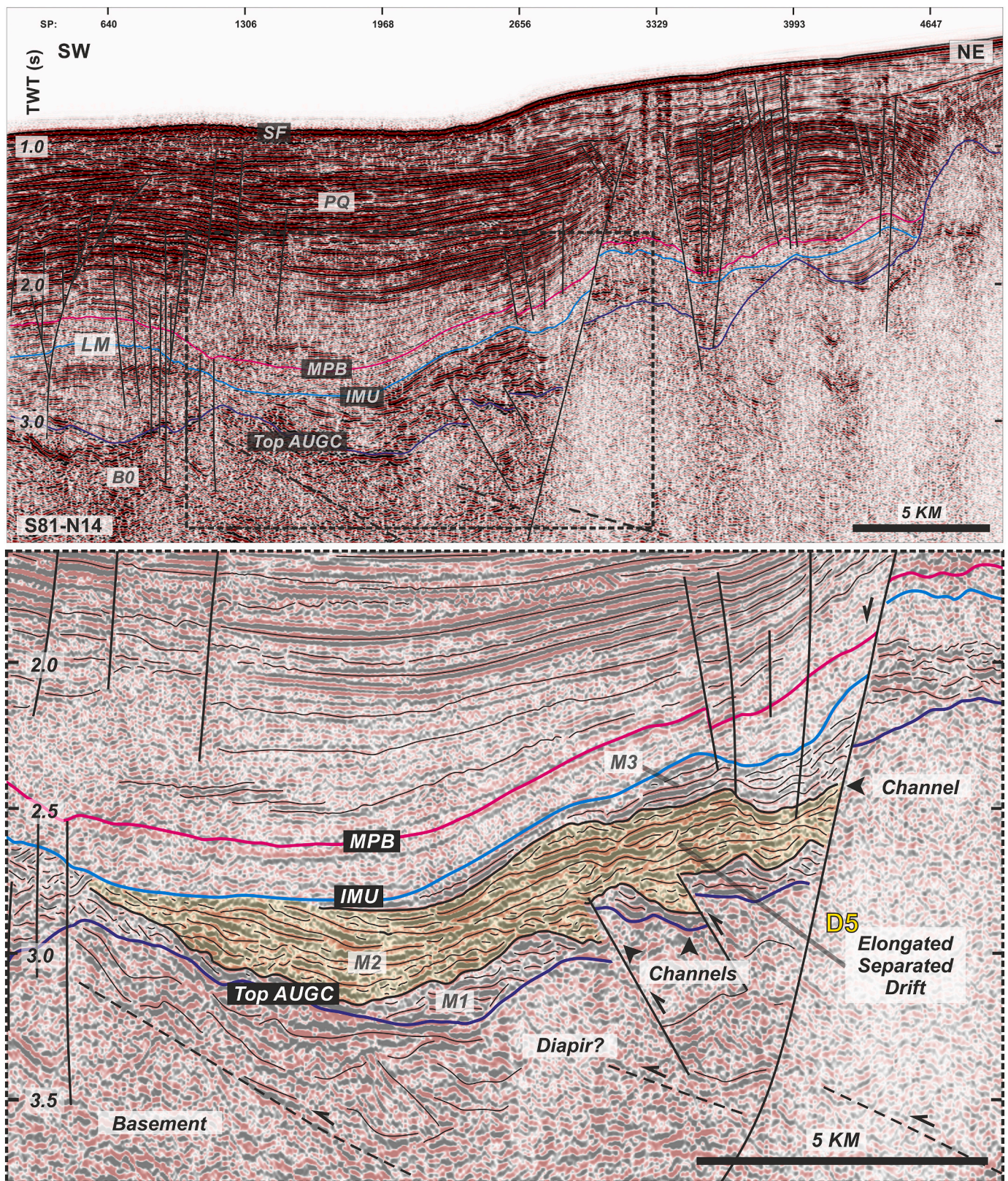


Fig. 11. Seismic profile in Cádiz basin (CB), Southwest Iberian margin (S81-N14) showing a mounded drift (D5) west of a fault scarp. Profile location given in Fig. 2. Major sequences (PQ, LM and B0), subunits of Lower LM (M3, M2 and M1) and main boundaries or discontinuities (SF: seafloor; other abbreviations given in Fig. 4; red arrows: stratal terminations). (For interpretation of the references to colour in this figure legend, the reader is referred to the web version of this article.)

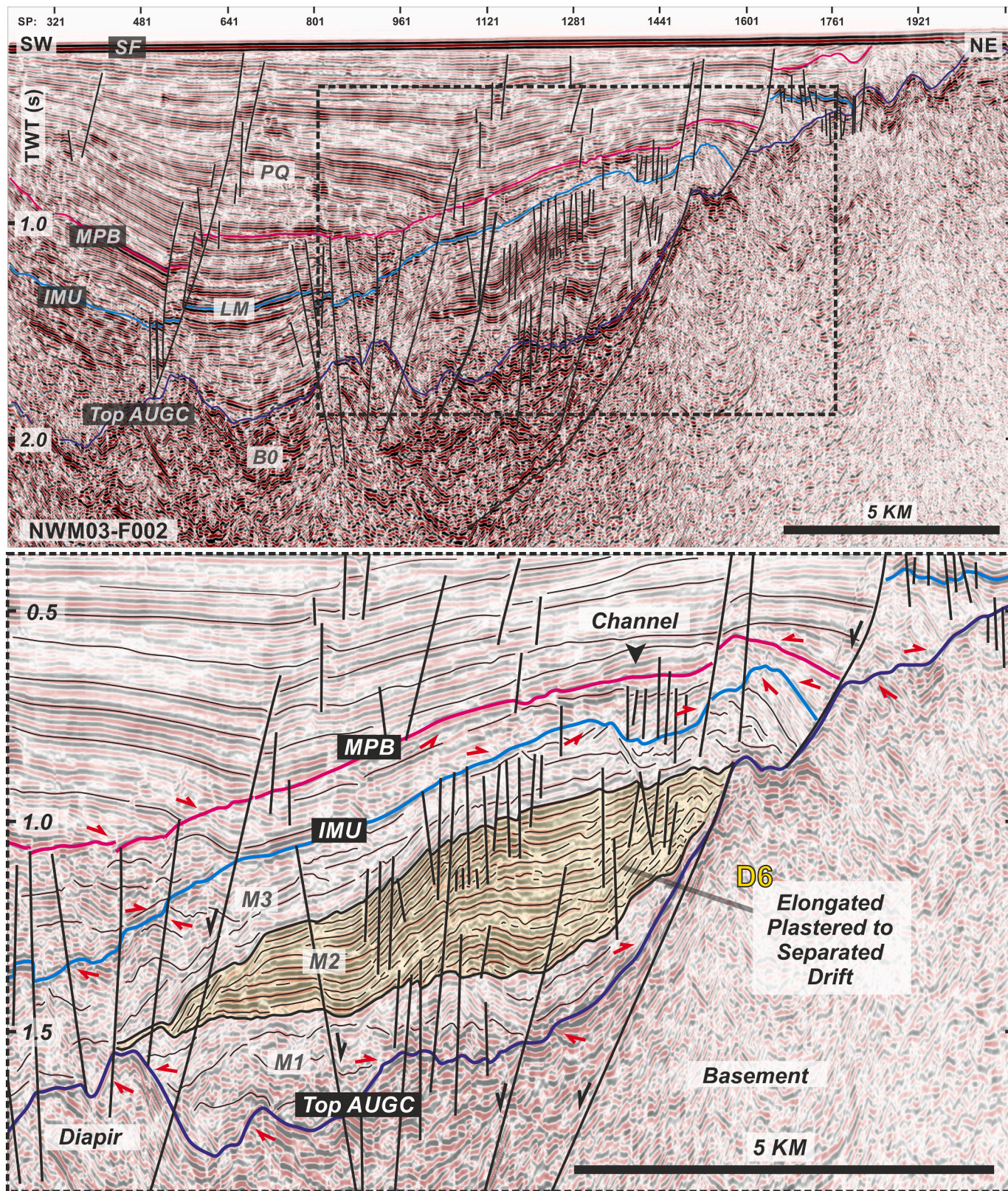


Fig. 12. Seismic profile in eastern Offshore Gharb basin, Northwest Moroccan margin (NWM03-F002) showing a plastered to mounded drift (D6) west of a fault scarp. Profile location given in Fig. 2. Major sequences (PQ, LM and B0), subunits of Lower LM (M3, M2 and M1) and main boundaries or discontinuities (SF: seafloor; other abbreviations given in Fig. 4; red arrows: stratal terminations). (For interpretation of the references to colour in this figure legend, the reader is referred to the web version of this article.)

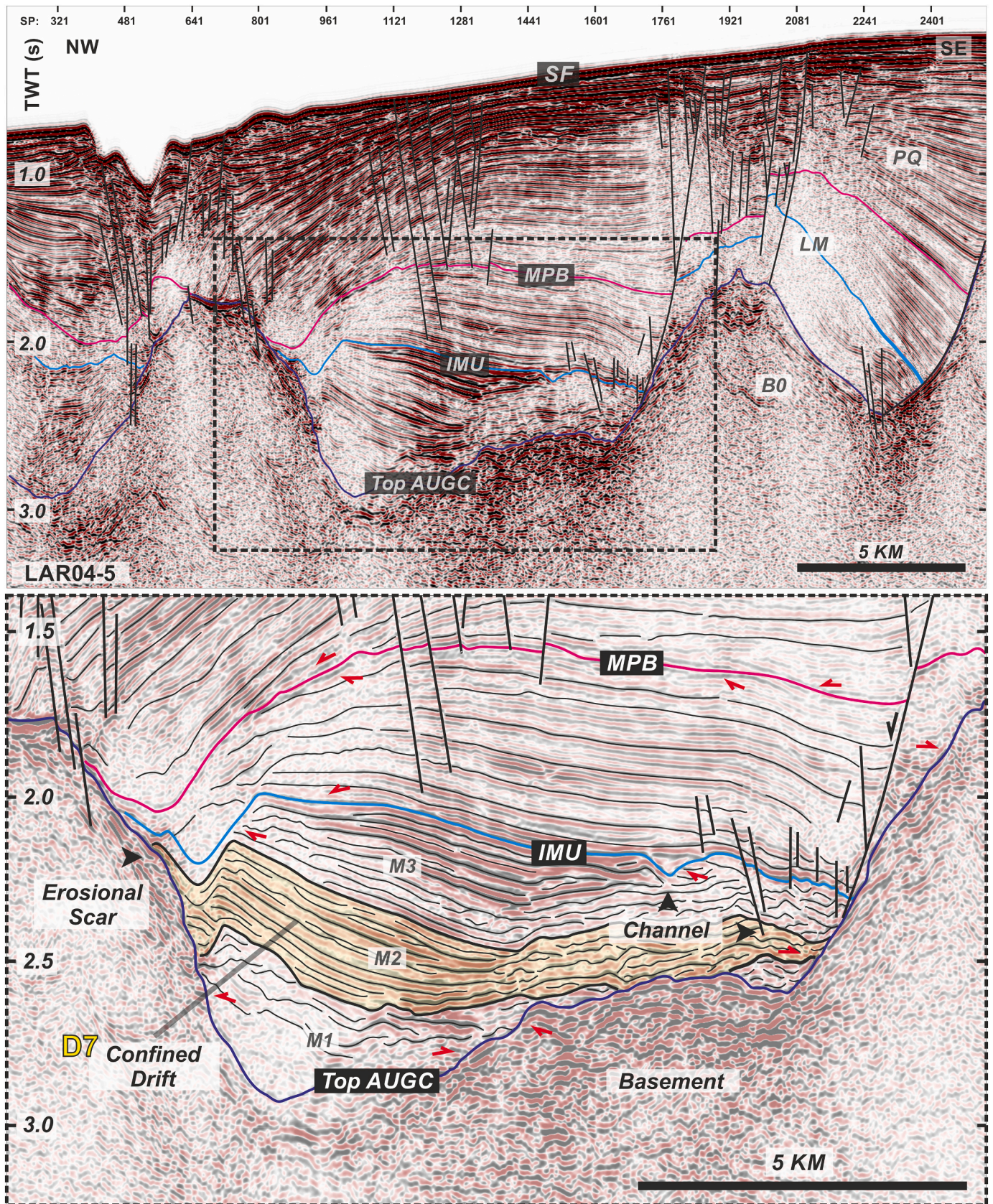


Fig. 13. Seismic profile in western Offshore Gharb basin, Northwest Moroccan margin (LAR04-5) showing an asymmetric confined drift (D7) bounded by basement highs and flanked by erosional scar and channels. Profile location given in Fig. 2. Major sequences (PQ, LM and B0), subunits of Lower LM (M3, M2 and M1) and main boundaries or discontinuities (SF: seafloor; other abbreviations given in Fig. 4; red arrows: stratal terminations). (For interpretation of the references to colour in this figure legend, the reader is referred to the web version of this article.)

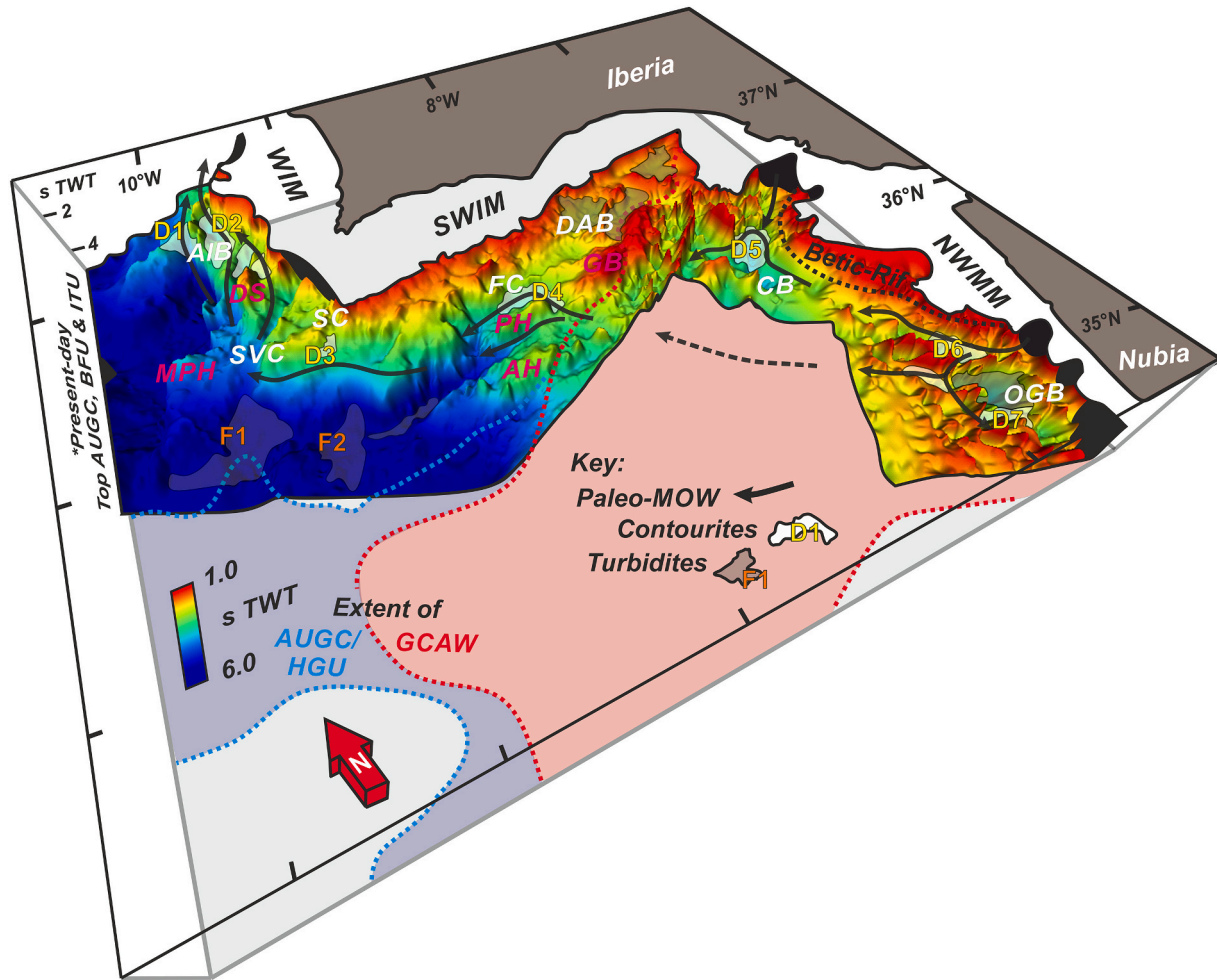


Fig. 14. Schematic model for the relationship between contourite distribution (Fig. 5a, D1-D7) and potential pathway of the paleo-Mediterranean Outflow Water (MOW) for the late Miocene Gulf of Cádiz CDS, superposed on the Base LM structure map (Fig. 6b) loosely representing the paleobathymetry of the late Miocene. (NWMM: Northwest Moroccan margin, SWIM: Southwest Iberian margin, WIM: West Iberian margin; other abbreviations given in Fig. 1).

Upper and Lower LM unit; and c) Pliocene to present (PQ) (Figs. 3 and 4). Their descriptions are summarised in Table 1.

The distribution of the seismic sequence LM, shown in Figs. 3 and 5, varies across the three different sectors, being thicker in the Cádiz and Offshore Gharb basin, averaging ~ 1 s TWT, and up to ~ 1.5 – 2 s TWT in the central part of the Offshore Gharb basin. This unit can also be found sparsely distributed within the middle slope of the offshore Betic foreland basin and the southern West Iberian margin on flatter slopes or terraces, or within canyons and valleys; otherwise it is only thinly draped over basement highs or truncated against the younger seismic unit PQ (Fig. 3). The presence (or absence) of the Lower LM unit is largely responsible for the variability of the distribution of seismic sequence LM across the different sectors, which can reach up to 0.5 s in the Betic foreland basin and the southern West Iberian margin, and over 1.0 s TWT in the Cádiz and Offshore Gharb wedge top basins (Fig. 5). The Lower LM unit is divided into sub-units of distinct seismic facies (Fig. 4). The basal surface of seismic sequence LM is represented by the combination of Top AUGC (allochthonous unit of the Gulf of Cádiz), BFU (basal foredeep unconformity) and ITU (intra-Tortonian unconformity) horizons in their respective sectors (Fig. 6b, 7-13). Above the basal surface, an older interval (sub-unit M1) of transparent or low-amplitude discontinuous to semi-continuous facies can be observed mainly in the

offshore Betic foreland and wedge top basins of the Gulf of Cádiz above the BFU or Top AUGC (Figs. 10-13). Similar facies are interspersed in the southern West Iberian margin above the ITU, in the basin centre or towards the lower slope (Figs. 7 and 8). Above sub-unit M1, a second interval (sub-unit M2) consists of two alternating high- to low-amplitude facies cycles, the lower section having a mounded geometry with continuous reflections and baselap or downlap terminations internally; it transitions into a top way to shingled or subparallel geometry for the upper section (Figs. 7-13). Sub-unit M2 directly overlies the ITU in some areas of the southern West Iberian Margin (Figs. 8-9). Towards the top of the seismic sequence LM, the younger interval (sub-unit M3) is truncated against the IMU (intra-Messinian unconformity) horizon. This sub-unit consists of bottom low amplitude semi-continuous to discontinuous facies transitioning upwards into top prominent high amplitude sub-parallel facies with wavy to sigmoidal reflections (Figs. 10, 12-13). Channelised features developed along the flank of the basin margin are normally associated with this phase (Figs. 11-13). The overall geometry of sub-unit M3 is usually not captured as the top section may be absent in the basin margin, with only the lower section truncated against the IMU (Figs. 10-12). Where observed, sub-unit consists of a similar cyclic facies trend with a low amplitude base transitioning upwards to a moderate- to high- amplitude top (Figs. 10 and 13). In the basin centre, this phase,

represented by an elongated and lenticular or sheeted wedge at its top with an internal subparallel configuration with downlap and truncation, can be observed as relatively concordant with the overlying Upper LM unit (Fig. 13). The IMU horizon is marked by erosional truncation of the Lower LM unit (Figs. 7-13).

4.2. Seismic facies of the lower LM unit

Figs. 7 to 13 show some examples of seismic facies and geometries identified within the Lower LM unit. In the middle slope of the southern West Iberian margin, we identified a mounded geometry (~10 km long and ~0.3 s TWT thick, at ~2.5–2.8 s TWT) in the SW-NE oriented PD00–517 profile (Fig. 7) of the sub-unit M2 located on a flatter part of the slope on the western flank of a basement high (lower section of

seismic sequence B2) protruding above the seafloor. A channelised feature (~1 km wide and 0.15 s TWT deep), also seen on the present-day seafloor, separates the mounded feature from the basement high. The internal configuration of the mounded feature consists of subparallel reflections with baselap terminations against sub-unit M1 or the ITU above seismic sequence B2, proximal to the valley-shaped feature, whereas more obvious downlap terminations are observed in the distal part of the mound. Towards the top part of the mound, a minor unconformity separates an upper high amplitude section from the lower moderate to low amplitude section. The crestal part of the mound is also affected by faulting. Underlying sub-unit M1 is sparsely distributed along the distal part of the slope and truncates sub-unit M2, while overlying sub-unit M3 onlaps the northwestern side of the mounded geometry (Fig. 7). Below the ITU, a mounded geometry can also be

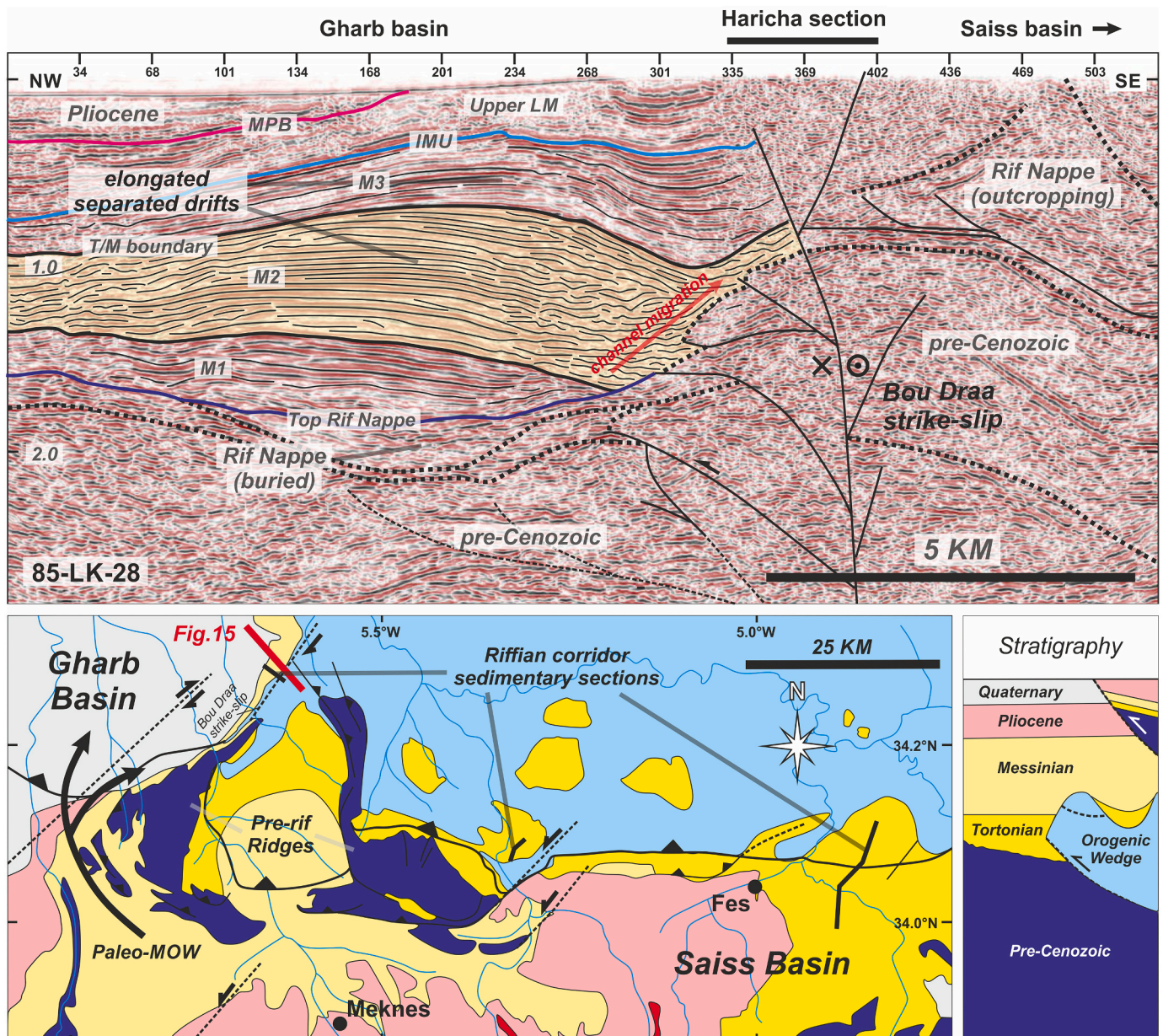


Fig. 15. (Top) Seismic profile in western Onshore Gharb basin, subsurface of the Haricha section (85-LK-28), showing the distribution of the Lower LM subunits (M3, M2 and M1), main boundaries and discontinuities, and the presence of elongated separated drifts associated with the late Miocene contourite depositional system in the Rifian corridor. Seismic interpretation adapted from Capella et al. (2017a, 2017b). (T/M boundary: Tortonian-Messinian boundary, other abbreviations available in Fig. 4); (Bottom) Simplified geological map of the Rifian corridor showing the location of seismic profile 85-LK-28 and sedimentary sections of the Rifian corridor late Miocene CDS, and the paleo-MOW pathway (adapted from Capella et al., 2017a, 2017b) (Location of section indicated in Fig. 1).

identified within the uppermost interval of seismic sequence B2, which had developed against the flank of the basement high (Fig. 7). Development of channel features was furthermore observed within the tabular sub-units M2 and M3 on the eastern flank of the basement high within a valley. Towards the base of the valley, the younger sub-unit M2 is deposited conformably on top of sub-unit M1 (Fig. 7).

In profile PD00–610 (Fig. 8), located in the Alentejo basin, we observed an elongated feature (~30 km long and ~0.15 s TWT thick, at 2.5–2.7 s TWT) with downlap terminations in the basal part (sub-unit M2) of a thinner Lower LM unit onto the ITU horizon. We likewise identified a channelised feature (~1 km wide and ~0.15 s TWT deep, at ~2.6 s TWT) scoured into the basal seismic sequence B2 along the base of the upper slope located E-NE of the drift. This feature dented a relatively flat ITU horizon towards the SW. Towards the distal part of the slope (W-SW), before the break into the abyssal plain, the reflection pattern evolves into ~10 km high amplitude long wavy geometries; they are more prominent in the upper section of sub-unit M2, which is equivalent to the top part of the mound, whereas the basal part consists of an older sub-unit M1 with transparent to low-amplitude reflections (Fig. 8).

Around Cape São Vicente, we identified fan geometries in the lower slope or continental rise to the Horseshoe abyssal plain (HAP) connected to the São Vicente and Sagres canyons (Fig. 5). São Vicente canyon develops in a NE-SW orientation through both seismic units PQ and LM. The N-S development of the Sagres canyon is more prominent in the seismic sequence LM interval than PQ. In the middle slope, Sagres canyon develops along the flank of the basement high in the east, cutting into seismic sequence B2 (Fig. 9). On the western flank of Sagres canyon, we identified in seismic profiles PD00–602 and 602A (Fig. 9) a mounded feature of sub-unit M2 with downlap terminations onto the ITU, building out to the west (up to ~5 km long and 0.2 s TWT thick, at 2–2.2 s TWT), which is in asymmetry with the eastern flank. The erosive IMU cuts into the thalweg of the canyon and is filled by the Upper LM unit. Distally from this structure towards the southwest, the Lower LM unit transitions upwards into wavy geometry on the lower slope. This is followed by a truncation termination against the IMU in a section with erosion or an absence of the Lower LM unit distribution (at 2.6–3.0 s TWT) and deposition of a growth wedge further towards the lower slope (Fig. 9).

Towards the western section of the Betic foreland basin, the thickest Lower LM unit interval (up to ~0.6 s TWT thick, at 2.5–3.1 s TWT) was found within Faro canyon, a valley (~0.6 s TWT deep) located west of the Deep Algarve basin (Fig. 3b), which is observed in seismic profile PD00–707 (Fig. 10). The discordant relationship of the Lower LM and Upper LM units separated by the IMU make geometrical interpretation of the upper sub-unit M3 interval unclear. Still, its internal configuration can be observed as low-amplitude discontinuous facies transitioning upwards into high-amplitude subparallel facies. In the sub-unit M2 interval, we similarly observed two cycles of alternating low- to high-amplitude reflection. The bottom (older) section has a mounded geometry, while the overlying (younger) section features a wavy geometry (Fig. 10). The internal configuration of the top cross-stratified wavy geometry (~1.5–2 km long and ~0.15 s TWT thick, at ~2.8 s TWT) consists of shingled facies with a concordant depositional western side and a truncated erosional eastern side. We also observed a channel feature (~1 km wide) to the west of this interval, flanking an intrusive structure. The mounded feature in the bottom section (~10 km long and ~0.25 s thick, at ~2.8–3.1 s TWT) developed in an E-W direction. It correlates to a channel feature towards the eastern end of this section, with the underlying lower amplitude semi-continuous reflections (sub-unit M1) truncated against the channel. In contrast, sub-unit M1 below shows of an overall thin tabular to sheeted geometry (Fig. 10).

In the central Gulf of Cádiz, distribution of seismic sequence LM is concentrated along the front of the Betic and Rif chain of the Gibraltar Arc, mainly in the Cádiz and Offshore Gharb basins (Fig. 5). Here, the Lower LM unit is also truncated against the IMU, but with a very distinct change in seismic facies, in terms of continuity and amplitude, than a

transparent unit in the Upper LM unit. As seen in seismic profile S81-N14 (Fig. 11) situated in the Cádiz basin, the distribution of the Lower LM unit is thicker at the footwall of a normal fault structure, albeit discordant against the overlying units/sub-units. Within the Lower LM unit, we identified a high amplitude interval (M2, at ~2.5–3 s TWT) with a lower section comprising multiple smaller channels cutting into an older interval of discordant to chaotic reflections (sub-unit M1) formed at the foot walls of thrust faults above a diapir, that were cut by a younger listric fault (at ~2.9–3 s TWT); and an upper section with a mounded feature (~4 km long and ~0.1 s TWT thick) associated with a channel that developed against the hanging wall of the fault. Seismic profile NWM03-F002 (Fig. 12) from the Offshore Gharb basin just off the Rifian front (Fig. 1), similarly identified a higher-amplitude interval (sub-unit M2) but shallower at 0.9–1.5 s TWT associated with a fault, above an interval of transparent to low-amplitude semi-continuous discordant to chaotic reflection facies (sub-unit M1). In turn, sub-unit M2 (~7 km long and ~0.4 s TWT thick) comprise two cycles of alternating low- to high- amplitude reflections. The lower section features a mounded geometry with a basal boundary having downlap terminations and a top boundary truncated against the upper section. The upper section is elongated and pinches out towards the southwest, with a transition from lower-amplitude with downlap terminations at the bottom, to higher-amplitude at the top. In both localities, we identified, above the high amplitude interval (sub-unit M2), a channel geometry (~1.5–2 km wide) associated with an upper (sub-unit M3) interval that developed along the front of a structural high (Fig. 11).

To the west of the Offshore Gharb basin, we identified a depocenter for seismic sequence LM in the deeper section of the basin (~3 s TWT deep), reaching up to ~1.3 s TWT in thickness, as seen in seismic profile LAR04–5 (Fig. 13). Here we note a concordance between the Upper and Lower LM units. The Lower LM unit has a sheeted geometry (~7 km long and ~0.6 s TWT thick) in the basin centre, correlated to a deep channel (~0.2 s TWT); and an erosional scar in the northern margin off a diapiric high, separating it from the Lower LM unit. The top interval (sub-unit M3) of this unit consists of lower amplitude reflections transitioned into prominent high-amplitude reflections with a wedge shape at the top (~0.2 s TWT thick), capped by the IMU. We also identified smaller channels (~0.5–1 km wide) developed along the southern margin. The sub-unit M2 interval consist of a lower section with parallel facies having onlap or truncation terminations, respectively against the northern diapir or channel, that transitioned upwards into subparallel reflections with internal stratal terminations. Sub-unit M2 overlies a sub-unit M1 interval having transparent to low-amplitude semi-continuous discordant to chaotic facies.

5. Interpretation

5.1. Distribution of the late Miocene contourite depositional system

We interpret some of the larger seismic geometries identified within the Lower LM unit of the Gulf of Cádiz as large depositional, erosional, and mixed features related to a regional late Miocene contourite depositional system (CDS) (Figs. 5 and 14).

In the southern West Iberian reactivated passive margin, the mounded feature observed within sub-unit M2 (Fig. 7) is interpreted as an *elongated separated drift* (D1) associated with an adjacent NE-SW *contourite channel (moat)* that developed under a north-easterly bottom current direction (Figs. 5 and 14), flowing on the western flank of the Príncipes de Avis seamount (PAS; Figs. 1 and 7). This interpretation conforms to the classification of drifts and inferred bottom current flow pattern in the northern hemisphere put forth by Faugères et al. (1999). The morphology of upper sub-unit M3 is unclear, given the erosional IMU (intra-Messinian unconformity) at the top (Fig. 7). While sub-unit M3 onlaps on the western side of the M2 mounded drift, separated by an unconformity, the development of the *channel* along the flank of the seamount during the deposition of sub-unit M3 is more pronounced

(Fig. 7). The mounded feature identified below the ITU (intra-Tortonian unconformity) in seismic sequence B2 is likewise viewed as an elongated separated drift, but older in age (Oligocene-Eocene to early middle Miocene?) separated by an erosional hiatus across the ITU, though its interpretation lies beyond the focus of this study (Fig. 7). On the eastern flank of the Príncipes de Avis seamount, *contourite channels* developed at the same time as the sub-unit M2 and M3 within the western margin of the Sines Pass valley, which acts as a depocenter during the deposition of the Lower LM unit (Figs. 5-7, 14). Within the Alentejo basin, we interpret the basal feature of sub-unit M2 (Fig. 8) as an *elongated separated drift* (D2) and a NW-SE *contourite channel (moat)* developing alongslope, located adjacent to the base of the upper slope, owing to a north-westerly bottom current direction (Figs. 5 and 14), following the drift classification and inferred bottom current directions of Faugères et al. (1999). The drift transitions into sediment waves towards the distal part of a *terrace* on the middle slope. Towards the top, sub-unit M3 is separated from sub-unit M2 by an unconformity and is eroded by the IMU (Fig. 8).

Further south off Cape São Vicente, we interpret the fan geometries connected to the São Vicente and Sagres canyons in the lower slope to continental rise as submarine fans (F1 & F2; Fig. 5), controlled by southward downslope depositional processes. On the middle slope region of this area (Fig. 9), the mounded deposits on the western flank of the Sagres canyon are interpreted as an asymmetric levee on the flanks of the Sagres canyon associated with the occurrence of a *mixed or hybrid system* (D3). This could happen as a result of short lateral diversion of the turbidity current by a westward flowing bottom current (Figs. 5 and 14), creating *asymmetric levees* as described by Menard (1955) and Miramontes et al. (2020); or further transport of sediment capture of the tail of the turbidity current by the bottom current to form the levee or drift body; or else winnowing or cleaning by the paleo-Mediterranean Outflow Water (MOW) to form bottom current reworked turbidite deposits within the channels (e.g., de Castro et al., 2020). The Sagres canyon became inactive in the middle to late Messinian, its development terminated by the IMU, and its thalweg filled by the Upper LM unit (Fig. 9). Further down the slope, the wavy geometry and erosional features that developed WNW-ESE alongslope are respectively interpreted as *sediment waves* and an *erosional scour* due to the westward flowing bottom current, bounded at the top by the IMU (Fig. 9). The features are thought to be deposited within sub-unit M2 overlying the ITU, while extensive erosion of the slope marked by the IMU could have removed sub-unit M3.

Towards the Southwest Iberian margin, the distribution of the contourite features is most prominent within the Faro canyon in the west, owing to its deeper local palaeotopography in the late Miocene in comparison to the Deep Algarve basin, hence providing accommodation for the deposition of the Lower LM unit (Figs. 5 and 6b). We interpret the top wavy and bottom mounded features identified within Faro canyon for sub-unit M2 as the development of a *confined drift* (D4), according to the classification of Faugères et al. (1999), that transitioned upwards into *sediment waves* (Fig. 10). The drift deposition is confined within Faro canyon by the slope face in the east and a diapir in the west, resulting in the development of *channels* on either side of the drift because of a northerly bottom current direction (Fig. 10). Sub-unit M2 is capped by an unconformity, underlying sub-unit M3. At the top of the upper sub-unit M3, the high amplitude continuous reflections to the east at the top of the interval may indicate more pronounced bottom current activity towards Messinian times, although the erosion marked by the IMU impedes interpretation of the seismic geometry for this sub-unit (Fig. 10).

Meanwhile towards the central Gulf of Cádiz and above the wedge top basins, an *elongated separated drift* (D5) and an *elongated plastered to separated drift* (D6) are respectively interpreted for the mounded features with high amplitude reflections identified in sub-unit M2 for the Cádiz and Offshore Cádiz basins (Figs. 11 and 12), based on the classification of Faugères et al. (1999). The location of this contourite drift is associated with faults or structural highs, where bottom currents would be

enhanced in a northward direction along the hanging wall or the flank of the high, located in the eastern margin of the basin (Figs. 5 and 14). In the Cádiz basin, we propose that *contourite channels* were formed by thrust faults linked to a decollement associated with the emplacement of the accretionary wedge (GCAW) but were later displaced by a listric fault caused by the gravitational collapse (Fig. 11). The local enhancement of bottom current could also be constrained by diapiric structures, which might have further strengthened current erosivity and its capacity in the scouring of channels. In turn, in the Offshore Gharb basin, drift deposition evolved from a basal separated drift to a plastered drift (D6) at the top of sub-unit M2, within accommodation caused by the normal listric fault (Fig. 12). This contourite drift is distinguished from pure growth strata features in extensional rollover systems (as in the upper LM and PQ units) given the mounded geometry of the deposits as well as the configuration of the reflection terminations against the fault scarp. Just above the sub-unit M2, sub-unit M3 shows a lower-amplitude reflection (Figs. 11 and 12), but it is partially eroded at its top, marked by the IMU. Contourite channels interpreted from the along-slope development of these channelised features of sub-unit M3 (Fig. 12) indicate a stronger influence of bottom currents towards the end of the Lower LM unit, albeit a transition to low amplitude seismic facies at the lower part of sub-unit M3.

Towards the western part of the Offshore Gharb basin, a continuous section of the seismic sequence LM could be identified (Fig. 13). We interpret the succession as a *confined drift* (D7), again according to Faugères et al. (1999), associated with *contourite channels* in the northwest and southeast having a westward bottom current direction (Figs. 5 and 14). The drift is asymmetrical with a skew towards the main channel in the northwest. The erosion of the channel is less prominent for sub-unit M2 with an internal erosive surface and capped by a minor unconformity (Fig. 13), thus indicating a more spread-out bottom current affecting the depocenter. The erosional scouring created a deeper channel for sub-unit M3, associated with a wedge-shaped deposit at the top of the drift and channelisation in the SE margin, indicative of a more focused and enhanced bottom current. These features associated with drift D7 are analogous to those of the late Quaternary contourite drift observed in the Doñana basin (Hernández-Molina et al., 2016).

6. Discussion

6.1. Stratigraphic and chronologic framework

The seismic stratigraphy of the Gulf of Cádiz is summarised in Fig. 4 and Table 1, and the seismic sequence LM is discussed in detail here. For the basal surface of the Lower LM unit, the basal foredeep unconformity (BFU) is documented as ~8 Ma (Maldonado et al., 1999), whereas the age for the intra-Tortonian unconformity (ITU) is speculative due to a lack of chronological information. We assume an age between ~7–8 Ma for the ITU, which correlates to the timing of final emplacement of the allochthonous units towards the northwest of the Gulf of Cádiz (Gràcia et al., 2003). This could have led to the thinner distribution or absence of the lowermost section of the Lower LM unit (sub-unit M1) to the northwest. The distribution of the upper Tortonian to lower Messinian Lower LM unit of the seismic sequence LM (~8–~6.4 Ma) is also dependent on the erosion and hiatus associated with the intra-Messinian unconformity (IMU, ~6.4 Ma; Ng et al., 2021) in different parts of the basin. Its deposition is controlled by the paleotopography of the underlying units, distinct in its respective sectors (seismic units B0, B1 and B2) (Fig. 6b; Table 1). Only a handful of boreholes are available for the correlation of the late Miocene succession. The GCMPC-1 well, located in the Cádiz basin (Fig. 2), penetrated the deep-marine Lower LM unit, but did not reach the allochthonous unit (AUGC) or the accretionary wedge (GCAW). The M1/M2 boundary correlates to fluctuations in the geophysical logs, with increases in spontaneous potential (SP) and gamma ray (GR), while the M2/M3 boundary correlates to a slight lithological change, the lower section becoming siltier and more

fossiliferous, with occasional micritic or oolitic limestone beds and traces of coal (Hernández-Molina et al., 2014). The wells Anchois-1, Deep Thon-1 and Merou-1 also penetrated the late Miocene succession in the Offshore Gharb basin. In the Deep Thon-1 and Merou-1 well, the Lower LM unit is dominated by distal turbidite channels, lobes or basin plain deposits, possibly reworked by later turbidity currents and or bottom currents (Ng et al., 2021). Upwards, the IMU horizon (~6.4 Ma) correlates to biostratigraphic events such as the Last Regular Occurrence (LRO) of *Globorotalia miotumida*, replaced by the First Occurrence (FO) of *Globorotalia margaritae*, dated 6.31–6.35 Ma, identified within a section of light grey clays interspersed with silts and very fine unconsolidated sands at the base of the Upper LM unit (Hernández-Molina et al., 2014; Ng et al., 2021). Still, the magnitude of this erosional hiatus is not known, as high-resolution biostratigraphic data below this boundary are lacking. We therefore postulate an age of ~6.6–6.4 Ma, inferred from the disappearance of paleo-Mediterranean Outflow Water (MOW) in the Onshore Gharb basin (Ivanovic et al., 2013). Above the Lower LM unit, the Upper LM unit is represented by the middle to upper Messinian unit of Ng et al. (2021) and the uppermost part of the U1 unit in Rodrigues et al. (2020). This unit correlates to a period dominated by pelagites or hemipelagites of the middle to late Messinian (~6.4 to 5.33 Ma; Ng et al., 2021). The background sediments are interrupted by gravity flow deposits, most prominently in the Deep Algarve and Offshore Gharb basins (Ng et al., 2021). On the basis of the Anchois-1 well, the Upper LM unit would consist of stacked channel storeys or complexes separated by thick hemipelagic drapes (Ng et al., 2021). Overall, seismic sequence LM reflects the late Miocene contourite depositional system.

6.2. Evolution of the late Miocene contourite depositional system

The long-term evolution of the late Miocene contourite depositional system (CDS) can be divided into three stages (*initial-, growth-, and maintenance-drift*) based on the morphology of the contourite features identified, followed by a final (*buried-drift*) stage representing the cessation of the system.

6.2.1. Initial-drift stage

At the base of the Lower LM unit, the predominantly transparent to low amplitude semi-continuous sub-unit M1 is interpreted as the *initial-drift stage* of the late Miocene CDS, which is marked by the onset of paleo-Mediterranean Outflow Water (MOW) during the late Tortonian above the BFU (~8 Ma). The sheeted to tabular distribution of sub-unit M1 in Faro Canyon (Fig. 10) and the Sines Pass in the southern West Iberian margin (Fig. 7) may have been originated by weak bottom current prior to the deposition of the more pronounced contourite features in sub-unit M2. This stage is comparable to the early Pliocene weak MOW phase observed for seismic sequence PQ, or Pliocene-Quaternary CDS (Hernández-Molina et al., 2016). The deposition of sub-unit M1 could also be synchronous with the emplacement of new imbricate wedges in the Gharb-Saïss basin, also known as the Prerifian Nappe [*sensu* Levy and Tilloy, 1962; as the equivalent to the allochthonous unit of the Gulf of Cádiz (AUGC) in the Rifian corridor (Flinch, 1993)], from ~8.4 to 7.8 Ma, just before the onset of contourite deposition in the Rifian Corridor (Capella et al., 2017b; de Weger et al., 2020). This is supported by the presence of deformed sub-unit M1 in the wedge top basins in the central Gulf of Cádiz above the Top AUGC (Figs. 11–13). The emplacement of the accretionary wedge and the gravitational collapse in the wedge top basins (Medialdea et al., 2004) prior to during this stage created the bathymetric control and accommodation for the evolution of the late Miocene CDS. The southern West-Iberian margin is likewise affected by the tectonic reactivation caused by an inversion of rift-related faults that uplifted the margin (Zitellini et al., 2004; Pereira et al., 2011). The sparse distribution of sub-unit M1 following the Miocene hiatus, represented by the ITU horizon in the Alentejo basin, corroborates this hypothesis.

6.2.2. Growth-drift stage

The *growth-drift stage* is represented by the sub-unit M2 interval, which consist of well-defined contourite drifts throughout the Gulf of Cádiz continental margins. More pronounced erosional and depositional features of the late Miocene contourite depositional system, such as mounded drifts and contourite channels, first developed after the onset of sub-unit M2 (Figs. 7–13). This represents an increase in the paleo-MOW velocity as it flows towards the Gulf of Cádiz, the outflow evolving into an overflow setting as suggested by Capella et al. (2019). Meanwhile, tectonic activity extending into the latest Tortonian (7–8 Ma; Gràcia et al., 2003) in the wedge top basins would have continued to create accommodation for drift growth. The base of sub-unit M2 is coeval with the onset of the sandy contourites succession described for the Rifian Corridor, which began between 7.8 Ma until 7.25 Ma during a period of relative tectonic quiescence (Capella et al., 2017a; de Weger et al., 2020). The boundary between sub-unit M2 and the overlying sub-unit M3 is marked by a minor unconformity and a shift from the high-amplitude top M2 interval to a low-amplitude bottom M3 interval. This could be attributed to an abrupt weakening or a change in pathway of the paleo-MOW and may further be related to a regional-scale event for the external wedges of the Gibraltar Arc during the Tortonian to Messinian (Abbassi et al., 2020). In the Rifian corridor onshore Morocco, a compressional tectonic event dated 7.25 Ma (Tortonian-Messinian boundary), linked to the transition from a thin- to thick-skinned tectonic regime for the Betic-Rif orogeny, is identified as the termination of a contourite depositional sequence in the Saïss basin (Capella et al., 2017b; de Weger et al., 2020); younger contourite deposits (~6.4–7.25 Ma) are also identified in the Onshore Gharb basin (Capella et al., 2017a). This event might have been responsible for the transition at the M2/M3 boundary. The Tortonian-Messinian boundary is moreover regarded as the initiation of the stepwise restriction of the Mediterranean-Atlantic exchange in the framework of a changing Mediterranean deep-water environment (Flecker et al., 2015).

6.2.3. Maintenance-drift stage

Sub-unit M3 is sparsely distributed from the Gulf of Cádiz to the southern West Iberian margin, due to an erosional phase post-deposition marked by the IMU during the early to middle Messinian (~6.4 Ma; *sensu* Ng et al., 2021). Sub-unit M3 transition upwards from low-amplitude reflections to very high-amplitude reflections, where deeply erosive alongslope contourite channels can be identified until the IMU (Figs. 8 and 12–13). In addition, contourite drift morphologies are observed only in the upper part of the sub-unit, being most obvious in the Offshore Gharb basin (Fig. 13). The evolution in the channel geometry and the change in drift morphology from subunit M2 to M3 in the western part of the Offshore Gharb would indicate an overall strengthening of the paleo-MOW. This is in agreement with the evolution of late Miocene CDS in the Rifian Corridor, where the paleo-MOW overflow is enhanced before its cessation (Capella et al., 2019). Therefore, we interpret sub-unit M3 as the *maintenance-drift stage* of the late Miocene CDS, similar to the present-day setting of the Pliocene-Quaternary CDS (Hernández-Molina et al., 2016).

6.2.4. Buried-drift stage

Subunit M3 is capped by the IMU, a tectonic episode witnessing the margin-wide erosion of the upper parts of subunit M3, plus a hiatus that lasted from ~6.6–6.4 Ma. The Upper LM unit is interpreted as the *buried-drift stage*, following the cessation of the paleo-MOW from ~6.4 Ma onwards, owing to the restriction of water exchange between the Mediterranean and the Atlantic due to uplift caused by the Betic-Rif orogeny, as well as the closure of the Betic and Rifian gateways (Krijgsman et al., 2018). This meant a switch from a contouritic to a predominantly pelagic or hemipelagic environment from the middle-late Messinian until the end of the Miocene (Ng et al., 2021). This stage is characterised by the inactivity of the contourite channels and their eventual and filling up by pelagic settling, along with the fossilization of the remaining drift

deposits which were unaffected by the IMU erosional unconformity. In the Offshore Gharb basin, the presence of thick hemipelagic drapes in between the turbiditic channel storeys or complexes further corroborates an absence of bottom currents at this time (Ng et al., 2021).

6.3. Control factors

The evolution of the late Miocene contourite depositional system (CDS) is controlled by the interplay between tectonic, sedimentary, and climatic forces.

6.3.1. Deformation from tectonism and diapirism

During the late Miocene, the formation of the elongated wedge top basins, such as the Cádiz and offshore Gharb basins, created relatively deeper passages for the paleo-MOW through the central part of the Gulf of Cádiz, that is, in comparison to the foredeep basins at the front of the Southwest Iberian and Northwest Moroccan margins (Figs. 3 and 5). The tectonic transformation of the Mediterranean-Atlantic gateways would have led to an increase in salinity and density for the outflowing paleo-MOW through the Betic and Rifian corridors (Capella et al., 2019), and sinking towards the deeper wedge top basins, driven by the density and mixing with ambient water before reaching neutral buoyancy west of the Doñana basin. In the *initial-drift stage*, the distribution of the highly deformed sub-unit M1 in the wedge top basins of the Gulf of Cádiz reflected the complex *syn*-tectonic depositional processes during this period (Figs. 12–13). Gravitational collapse and AUGC development, in addition to diapirism, disrupted and controlled the synchronous deposition of the sub-unit M1. At the southern West Iberian margin, continuous uplift due to tectonic inversion up to the late Tortonian could have led to erosion and an intersperse distribution or lack of preservation of the *initial-drift stage* (Figs. 7 and 8). The occurrence of larger and more mounded drift morphologies pertaining to the *growth*- and *maintenance-drift* phases in sub-units M2 and M3 would also be a result of morpho-tectonic activity exerting control on the confinement of bottom current pathways. The dimensions of the drift geometries within the central Gulf of Cádiz wedge top basins for the late Miocene are relatively small (<7 km in width) when compared to drifts in the southern West Iberian margin (10–30 km wide) or the Deep Algarve basin Pliocene-Quaternary drifts (40–50 km wide; Hernández-Molina et al., 2016). The smaller late Miocene drifts reflect how the effects of bathymetric irregularities caused by tectonism and diapirism during this period conditioned both drift morphologies and distributions. As a result of the tectonic processes, basement highs, fault scarps and diapiric structures (salt domes, salt walls) acted as obstacles that locally enhanced bottom current flow and formed erosional features (channels, scours) or deposited mounded drifts with coarser sediments, controlling and confining the distribution of the late Miocene CDS from the Gulf of Cádiz to the southern West Iberian margin (Figs. 10–13). The effects of these bathymetric features in enhancing MOW has also been documented in the Pliocene-Quaternary CDS (Sánchez-Leal et al., 2017; Duarte et al., 2020).

6.3.2. Interplay of turbidity and bottom currents

Deposition of the late Miocene CDS was also controlled by the interaction of alongslope and downslope sedimentary processes. Gravitational deposits over the continental margins were reworked by the paleo-MOW flowing across the Gulf of Cádiz during the late Miocene. Examples of downslope processes during this period include the turbiditic systems within the Deep Algarve and Offshore Gharb basins (Fig. 3; Ng et al., 2021), and the formation of the Sagres and São Vicente submarine canyons in the southern West Iberian margin (Fig. 5). Reworking of these gravity flow deposits by the paleo-MOW bottom currents would have produced mixed or hybrid systems (Mulder et al., 2008; Rodrigues et al., 2021). Yet, a paleo-Portimão submarine canyon (Figs. 5–6) controlled by the Gil Eanes fault zone (GEF; *sensu* Duarte et al., 2020) could have supplied sediments for drift development in Faro canyon. In the offshore Gharb basin, the presence of bottom-currents could rework

the dominantly turbiditic environment, giving rise to bottom-current reworked sands and contourite drifts (Shanmugam, 2008). Recent research in the Gulf of Cádiz underlines the complexity of the relationship between the two processes: MOW bottom currents and gravity flows (mass transport and turbidity currents), in the context of the Pliocene-Quaternary CDS (Brackenkridge et al., 2013; de Castro et al., 2020, 2021; Mencaroni et al., 2020; Mestdagh et al., 2020; Serra et al., 2020). The interaction of different sedimentary processes in the deposition of contourite drift is well demonstrated in the analyses of core, log and seismic scales for the Pliocene to Quaternary interval (Brackenkridge et al., 2013; de Castro et al., 2021; Mestdagh et al., 2020); the influence of the MOW on the São Vicente submarine canyon has also been documented (Mencaroni et al., 2020; Serra et al., 2020).

6.3.3. Orbital and millennial variability

Some examples of the late Miocene drift features evoke cyclicities previously identified for the Pliocene-Quaternary CDS (Llave et al., 2001; Hernández-Molina et al., 2016; Figs. 10 and 13). These cyclic seismic facies trend with a transparent base, parallel reflectors of moderate-to-high amplitude top, and capped by a continuous high-amplitude erosional surface are here interpreted as a coarsening-upward sequence linking MOW variability with orbital cycles (Hernández-Molina et al., 2016). The sub-unit scale cyclicity could be influenced by the Milankovitch precession cycles modulated by eccentricity cycles, which are thought to have an influence on sea-level variation, sediment supply, and bottom current activity, according to seismic and sequence stratigraphic analysis of the Pliocene-Quaternary CDS in the Gulf of Cádiz (Hernández-Molina et al., 2016; Mestdagh et al., 2019). The termination of the late Miocene CDS also took place coevally to both tectonic and sedimentary changes influenced by orbital cycles. This margin-wide erosive event coupled with increasing turbidite deposition, and the subsequent pelagic environment across the Gulf of Cádiz, marked the weakening and eventual cessation of paleo-MOW driven by the uplifting and shallowing of the sills within the Betic and Rifian corridors (Krijgsman et al., 1999; Ng et al., 2021). The event is furthermore linked to the stepwise restriction of the Mediterranean-Atlantic connection, which is imprinted on long-term eccentricity orbital cycles (Hilgen et al., 2007; Ng et al., 2021). Variations in MOW strength are also observed at the smaller precessional to millennial scale (Llave et al., 2006; de Castro et al., 2020; Sierro et al., 2020). High-amplitude facies are represented by coarser-grained sediments, deposited during precession maxima or Greenland stadials, where enhancement of the MOW would be a result of aridity and increased buoyancy loss in the eastern Mediterranean (Sierro et al., 2020). During Heinrich stadials, increasing strength and a deepening of the MOW towards the lower core, along with decreasing MOW strength in the upper core, would entail freshening of the Atlantic and increased density contrast with the MOW (Llave et al., 2006; Sierro et al., 2020). Such climatic-induced effects can also be seen in the intermittent behaviour of the paleo-MOW as it controls the deposition of late Miocene contourites in the Rifian corridor (de Weger et al., 2020).

6.4. Implications of the late Miocene contourite depositional system

The long-term evolution of drift morphologies of the late Miocene contourite depositional system (CDS) shows similarities with other modern examples around the Iberian margin, such as the Gulf of Cádiz Pliocene-Quaternary CDS in the Southwest Iberian margin (Hernández-Molina et al., 2016); the Sines drift in the West Iberian margin (Rodrigues et al., 2020); and the Le Danois CDS in the Northern Iberian margin (Liu et al., 2020). These modern examples developed as a result of Pliocene to present-day setting of the Mediterranean Outflow Water (MOW) (Llave et al., 2019), where they reflect its evolution towards a denser and more restricted setting across the Strait of Gibraltar (Hernández-Molina et al., 2016). Similarly, the development of the late Miocene contourite depositional system acts as an imprint upon the

paleo-MOW circulation in the Gulf of Cádiz towards the southern West Iberian margin, where its different stages (*initial-*, *growth-* and *maintenance-drift*) trace the increasing density contrast between the Mediterranean and Atlantic throughout the late Miocene. The narrowing and subsequent closure of the Betic and Rifian corridors since the late Miocene led to the evolution of the paleo-MOW into an overflow setting with a more saline and denser water mass (Capella et al., 2019). Ultimately, the outflow was reduced or halted (Ng et al., 2021), followed by the partial isolation of the Mediterranean Sea and the precipitation of the Messinian salinity crisis evaporites during the late Messinian (Flecker et al., 2015). This transformation from an outflow to an overflow setting is also evident for the coeval deposition of contourites in the Rifian corridor (Capella et al., 2017a; de Weger et al., 2020). The late Miocene CDS, likewise identified by Capella et al. (2017a), is seen in the seismic profile subsurface of the Haricha section, at the eastern margin of the onshore Gharb basin by the exit of the Rifian corridor. Here, elongated separated drifts are interpreted for subunits M2 and M3 (*growth- and maintenance-drift stage*), while subunit M1 with its sheeted and tabular geometry, points to the *initial-drift stage* (Fig. 15).

The presence of the late Miocene CDS in the Gulf of Cádiz occurred during a period of tectonic deformation as a consequence of the ongoing progressive restriction of the Mediterranean-Atlantic gateway during the Tortonian to Messinian stages (Capella et al., 2017b) due to convergence of the Iberian and African plates leading to the uplift of the Gibraltar Arc (Duggen et al., 2003; Civiero et al., 2020). In contrast to other contourite systems, in this case tectonism and diapirism exerted greater control over the distribution and dimension of the deposits. The contourite drifts identified in the wedge top basins in the central Gulf of Cádiz (Figs. 11–13, 14) are concentrated in areas confined by structural highs or fault scarps that developed synchronously, through the emplacement of the accretionary wedge and the gravitational collapse during the middle to late Miocene (Medialdea et al., 2004; Gràcia et al., 2003). Drifts in the southern West Iberian margin though, are located on the flank of structural highs (Figs. 7–8, 14) resulting from the tectonic inversion and reactivation of rift-related faults and margin uplift (Zitellini et al., 2004; Pereira et al., 2011). Bathymetric features such as these would have locally accelerated bottom current flow (Sánchez-Leal et al., 2017; Duarte et al., 2020). The smaller dimensions of these drift deposits would also be restricted by the availability of accommodation. In the setting of the onshore Gharb basin, the late Miocene contourite drift subsurface of the Haricha section (Fig. 15), identified by Capella et al. (2017a), is deposited in similar settings, the deposits being locally bounded by structural highs created by emplacement of the Rif Nappe, as seen in both the seismic cross section and the geological map (Fig. 15). The overall preservation of contourite drift deposits would have been adversely affected in continental margins undergoing deformation processes such as uplift, where deposits of older stages are susceptible to widespread erosion by younger and more vigorous bottom currents. Distinguishment of the late Miocene CDS may serve as a good analogue for drift discrimination in other tectonically active settings.

The late Miocene CDS also provide insights as to the climatic and oceanographic history from the Tortonian to the Messinian. A weaker outflow of the paleo-MOW across a wide Mediterranean-Atlantic gateway might have existed during the middle- to early-late Miocene (Capella et al., 2019), prior to deposition of the *initial-drift stage*. Yet no evidence of such was preserved due to the tectonic activity and deformation in the Gulf of Cádiz towards the southern West Iberian margin. This outflow setting would have generated a distinctive water mass in the Atlantic and influenced the North Atlantic paleoceanography. The onset of the overflow setting of the paleo-MOW exchange during the late Miocene would have increased entrainment of ambient Atlantic water to form the paleo-Atlantic Mediterranean Water (AMW; Rogerson et al., 2012) and flowed towards the North Atlantic. This would have had a significant impact on the ocean circulation in the North Atlantic. The late Miocene Mediterranean overflow most likely helped to sustain the formation of the North Atlantic Deep Water (NADW) (Rogerson et al.,

2012) and the Atlantic Meridional Overturning Circulation (AMOC) (Rogerson et al., 2006; Ivanovic et al., 2013). Capella et al. (2019) similarly suggested that overflow conditions could have favoured ocean-atmospheric carbon dioxide (CO₂) decoupling by initiating an ocean pump for CO₂ transport. Such a scenario would have meant surface water cooling and carbon sequestration in the deep ocean (Capella et al., 2019), and contributed to the late Miocene global cooling trend (Herbert et al., 2016; Capella et al., 2019), hence the northern hemisphere Messinian ice ages (van der Laan et al., 2012).

7. Conclusion

A late Miocene contourite depositional system (CDS) in the Neogene basins across the middle slope of the Gulf of Cádiz was recognised through the documentation of drift deposits and erosional features which act as clues to the paleoceanographic imprints of bottom water circulation during the late Miocene. Here, we describe for the first time the occurrence of regional contourite features after the main emplacement of the accretionary wedge (GCAW) or allochthonous unit (AUGC) during the late Tortonian, prior to the disconnection of the Mediterranean-Atlantic exchange in the middle to late Messinian (~6.4 Ma). This supports the influence of paleo-Mediterranean Outflow Water (MOW) water mass in locally controlling the morphology and sedimentary stacking pattern on the middle continental slope of the Gulf of Cádiz and towards the southern West Iberian margin, downstream of the Betic and Rifian corridors. Seismic stratigraphic analysis served to identify the four stages related to the evolution of the late Miocene CDS, based on external morphological expressions and internal reflection configurations, namely the *initial-drift stage* (subunit M1), the *growth-drift stage* (sub-unit M2), the *maintenance-drift stage* (sub-unit M3), and the *buried-drift stage* (Upper LM unit). They record the weak to vigorous long-term evolution of the bottom current velocity and its subsequent halt in relation to the synchronous restriction of the Mediterranean-Atlantic gateway. The distribution and preservation of these contourite drifts are favoured by local *syn-* and *post-depositional* tectonic deformation. Locally, sediments within these drift deposits are supplied by downslope gravitational systems, whereas regional uplifting processes affects sediment erosion and accommodation, thereby contributing to the evolution of the overall drift morphology.

However, certain limitations of the seismic and borehole data impede a more detailed description of the sedimentary evolution of the CDS. Acquisition of 3D and reprocessing of 2D seismic data with a refined interpretation workflow, as well as the obtainment of sedimentological information from boreholes in the study area, would be necessary to unravel, with higher confidence, the role of bottom currents in controlling the sedimentary stacking patterns, and their interaction with other deep-water processes in depositing the late Miocene CDS. Proxies for climatic and tectonic changes are also vital to explain their effects on the local and regional scale. The upcoming IMMAGE amphibious (IODP 895 and ICDP) drilling project (Investigating Miocene Mediterranean-Atlantic Gateway Exchange: <http://image.icdp-online.org>) will be able to provide the data to better understand the late Miocene CDS of the Gulf of Cádiz. Notwithstanding, this work marks a crucial step towards understanding the long-term evolution of the late Miocene Mediterranean-Atlantic exchange and the effect of the paleo-MOW evolution on ocean circulation in the North Atlantic, as well as its impact on late Miocene global climate cooling. The seismic analysis of the late Miocene CDS in the Gulf of Cádiz could also serve as an analogue for recognising highly deformed contourite deposits in the subsurface of other tectonically active continental margins.

Declaration of Competing Interest

The authors declare that they have no known competing financial interests or personal relationships that could have appeared to influence the work reported in this paper.

Acknowledgments

This work is conducted in the framework of “The Drifters” Research Group, Royal Holloway University of London and supported by Royal Holloway college studentship, SCORE (CGL2016-80445-R) and INPULSE (CTM2016-75129-C3-1-R) projects. Datasets are available from ONHYM, Repsol S.A., and TGS-NOPEC with confidentiality regulations, and are not publicly accessible. However, they are available from the authors upon reasonable request and permissions from ONHYM, Repsol S.A., or TGS-NOPEC. The authors would like to extend their grateful thanks to Mr. Mohamed Nahim as Director of Petroleum Exploration (ONHYM) for his support, and to ONHYM, Repsol S.A., and TGS-NOPEC for permission to use the seismic and borehole data in this work. We thank the editors and the two anonymous reviewers for their positive suggestions which help us to improve the manuscript.

Appendix A. Supplementary data

Supplementary data to this article can be found online at <https://doi.org/10.1016/j.margeo.2021.106605>.

References

- Abbassi, A., Cipollari, P., Zaghoul, M.N., Cosentino, D., 2020. The Rif Chain (Northern Morocco) in the late Tortonian-early Messinian Tectonics of the Western Mediterranean Orogenic Belt: evidence from the Tanger-Al Manzla Wedge-Top Basin. *Tectonics* 39. <https://doi.org/10.1029/2020TC006164> e2020TC006164.
- Ambar, I., Howe, M.R., 1979. Observations of the Mediterranean outflow-II. The deep circulation in the vicinity of the Gulf of Cadiz. *Deep-Sea Res.* 26A, 555–568. [https://doi.org/10.1016/0198-0149\(79\)90096-7](https://doi.org/10.1016/0198-0149(79)90096-7).
- Bailey, W.S., McArthur, A.D., McCaffrey, W.D., 2021. Distribution of contourite drifts on convergent margins: examples from the Hikurangi subduction margin of New Zealand. *Sedimentology* 68, 294–323. <https://doi.org/10.1111/sed.12779>.
- Brackenridge, R., Hernández-Molina, F.J., Stow, D.A.V., Llave, E., 2013. A Pliocene mixed contourite-turbidite system offshore the Algarve margin, Gulf of Cadiz: Seismic response, margin evolution and reservoir implications. *Mar. Pet. Geol.* 46, 36–50. <https://doi.org/10.1016/j.marpetgeo.2013.05.015>.
- Capella, W., Hernández-Molina, F.J., Flecker, R., Hilgen, F.J., Hssain, M., Kouwenhoven, T.J., van Oorschot, M., Sierro, F.J., Stow, D.A.V., Trabucho-Alexandre, J., Tulbure, M.A., de Weger, W., Youfi, M.Z., Krijgsman, W., 2017a. Sandy contourite drift in the late Miocene Rifian Corridor (Morocco): reconstruction of depositional environments in a foreland-basin seaway. *Sediment. Geol.* 355, 31–57. <https://doi.org/10.1016/j.sedgeo.2017.04.004>.
- Capella, W., Matenco, L., Dmitrieva, E., Roest, W.M., Hessels, S., Hssain, M., Chakor-Alami, A., Sierro, F.J., Krijgsman, W., 2017b. Thick-skinned tectonics closing the Rifian Corridor. *Tectonophysics* 710, 249–265. <https://doi.org/10.1016/j.tecto.2016.09.028>.
- Capella, W., Flecker, R., Hernández-Molina, F.J., Simon, D., Meijer, P.T., Rogerson, M., Sierro, F.J., Krijgsman, W., 2019. Mediterranean isolation preconditioning the Earth System for late Miocene climate cooling. *Sci. Rep.* 9, 3795. <https://doi.org/10.1038/s41598-019-40208-2>.
- Civiero, C., Custódio, S., Duarte, J.C., Mendes, V.B., Faccenna, C., 2020. Dynamics of the Gibraltar Arc System: A Complex Interaction Between Plate Convergence, Slab Pull, and Mantle Flow. *Journal of Geophysical Research: Solid Earth* 125. <https://doi.org/10.1029/2019JB018873> e2019JB018873.
- de Castro, S., Hernández-Molina, F.J., Rodríguez-Tovar, F.J., Llave, E., Ng, Z.L., Nishida, N., Mena, A., 2020. Contourites and bottom current reworked sands: Bed facies model and implications. *Mar. Geol.* 428, 106267. <https://doi.org/10.1016/j.margeo.2020.106267>.
- de Castro, S., Hernández-Molina, F.J., de Weger, W., Jiménez-Espejo, F.J., Rodríguez-Tovar, F.J., Mena, A., Llave, E., Sierro, F.J., 2021. Contourite characterization and its discrimination from other deep-water deposits in the Gulf of Cadiz contourite depositional system. *Sedimentology*. <https://doi.org/10.1111/sed.12813>.
- de Weger, W., Hernández-Molina, F.J., Flecker, R., Sierro, F.J., Chiarella, D., Krijgsman, W., Manar, M.A., 2020. Late Miocene contourite channel system reveals intermittent overflow behavior. *Geology*. <https://doi.org/10.1130/G47944.1>.
- Duarte, J.C., Rosas, F.M., Terrinha, P., Gutscher, M.-A., Malavieille, J., Silva, S., Matias, L., 2011. Thrust–wrench interference tectonics in the Gulf of Cadiz (Africa–Iberia plate boundary in the North-East Atlantic): insights from analog models. *Mar. Geol.* 289, 135–149. <https://doi.org/10.1016/j.margeo.2011.09.014>.
- Duarte, D., Roque, C., Hernández-Molina, F.J., Ng, Z.L., Magalhães, V.H., Llave, E., Sierro, F.J., 2020. Tectonic domains of the Betic Foreland System, SW Iberian margin: Implications for the Gulf of Cadiz Contourite System. EGU General Assembly 2020, Online, 4–8 May 2020, EGU2020-1033. <https://doi.org/10.5194/egusphere-egu2020-1033>.
- Duggen, S., Hoernle, K., van den Bogaard, P., Rüpke, L., Morgan, J.P., 2003. Deep roots of the Messinian salinity crisis. *Nature* 422, 602–606. <https://doi.org/10.1038/nature01553>.
- Expedition 339 Scientists, 2012. Mediterranean outflow: environmental significance of the Mediterranean Outflow Water and its global implications. IODP Preliminary Report 339. <https://doi.org/10.2204/iodp.pr.339.2012>.
- Faugères, J.-C., Stow, D.A.V., 2008. Continental drifts: Nature, evolution and controls. In: *Rebecco, M., Camerlenghi, A. (Eds.), Contourites. Developments in Sedimentology, vol. 60. Elsevier, Amsterdam, pp. 259–288.*
- Faugères, J.-C., Stow, D.A.V., Imbert, P., Viana, A., 1999. Seismic features diagnostic of contourite drifts. *Mar. Geol.* 162, 1–38. [https://doi.org/10.1016/S0025-3227\(99\)00068-7](https://doi.org/10.1016/S0025-3227(99)00068-7).
- Flecker, R., Krijgsman, W., Capella, W., de Castro Martíns, C., Dmitrieva, E., Maysner, J.P., Marzocchi, A., Modestou, S., Ochoa, D., Simon, D., Tulbure, M., van den Berg, B., van der Schee, M., de Lange, G., Ellam, R., Govers, R., Gutjahr, M., Hilgen, F.J., Kouwenhoven, T., Lofi, J., Meijer, P., Sierro, F.J., Bachiri, N., Barhoun, N., Chakor Alami, A., Chacon, B., Flores, J.A., Gregory, J., Howard, J., Lunt, D., Ochoa, M., Pancost, R., Vincent, S., Zakaria Youfi, M., 2015. Evolution of the late Miocene Mediterranean-Atlantic gateways and their impact on regional and global environmental change. *Earth Sci. Rev.* 150, 365–392. <https://doi.org/10.1016/j.earscirev.2015.08.007>.
- Flinch, J.F., 1993. Tectonic evolution of the Gibraltar Arc. Ph.D Thesis. Rice University, Houston. <https://doi.org/10.13140/RG.2.1.3898.6085>.
- García, M., Hernández-Molina, F.J., Llave, E., Stow, D.A.V., León, R., Fernández-Puga, M. C., Díaz del Río, V., Somoza, L., 2009. Contourite erosive features caused by the Mediterranean Outflow Water in the Gulf of Cadiz: Quaternary tectonic and oceanographic implications. *Mar. Geol.* 257, 24–40. <https://doi.org/10.1016/j.margeo.2008.10.009>.
- Gràcia, E., Dañoibeitia, J., Vergés, J., Bartolomé, R., 2003. Crustal architecture and tectonic evolution of the Gulf of Cadiz (SW Iberian margin) at the convergence of the Eurasian and African plates. *Tectonics* 22, 1033. <https://doi.org/10.1029/2001TC901045>.
- Herbert, T.D., Lawrence, K.T., Tzanova, A., Peterson, L.C., Caballero-Gill, R., Kelly, C.S., 2016. Late Miocene global cooling and the rise of modern ecosystems. *Nat. Geosci.* 9, 843–847. <https://doi.org/10.1038/ngeo2813>.
- Hernández-Molina, F.J., Llave, E., Preu, B., Ercilla, G., Fontan, A., Bruno, M., Serra, N., Gomez, J.J., Brackenridge, R.E., Sierro, F.J., Stow, D.A.V., García, M., Juan, C., Sandoval, N., Arnaiz, A., 2014. Contourite processes associated with the Mediterranean Outflow Water after its exit from the Strait of Gibraltar: Global and conceptual implications. *Geology* 42 (3), 227–230. <https://doi.org/10.1130/G35083.1>.
- Hernández-Molina, F.J., Llave, E., Somoza, L., Fernández-Puga, M.C., Maestro, A., León, R., Barnolas, A., Medialdea, T., García, M., Vázquez, J.T., Díaz del Río, V., Fernández-Salas, L.M., Lobo, F., Alveirinho Dias, J.M., Rodero, J., Gardner, J., 2003. Looking for clues to paleoceanographic imprints: a diagnosis of the gulf of Cadiz contourite depositional systems. *Geology* 31, 19–22. [https://doi.org/10.1130/0091-7613\(2003\)031<0019:LFCTPI>2.0.CO;2](https://doi.org/10.1130/0091-7613(2003)031<0019:LFCTPI>2.0.CO;2).
- Hernández-Molina, F.J., Stow, D.A.V., Llave, E., 2008. Continental slope contourites. In: *Rebecco, M., Camerlenghi, A. (Eds.), Contourites. Developments in Sedimentology, vol. 60. Elsevier, Amsterdam, pp. 379–408.*
- Hernández-Molina, F.J., Stow, D., Alvarez-Zarikian, C., Expedition IODP 339 Scientists, 2013. IODP Expedition 339 in the Gulf of Cadiz and off West Iberia: decoding the environmental significance of the Mediterranean outflow water and its global influence. *Sci. Drill.* 16, 1–11. <https://doi.org/10.5194/sd-16-1-2013>.
- Hernández-Molina, F.J., Sierro, F.J., Llave, E., Roque, C., Stow, D.A.V., Williams, T., Lofi, J., van der Schee, M., Arnáiz, A., Ledesma, S., Rosales, C., Rodríguez-Tovar, F. J., Pardo-Igúzquiza, E., Brackenridge, R.E., 2016. Evolution of the gulf of Cádiz margin and Southwest Portugal contourite depositional system: Tectonic, sedimentary and paleoceanographic implications from IODP expedition 339. *Mar. Geol.* 377, 7–39. <https://doi.org/10.1016/j.margeo.2015.09.013>.
- Krijgsman, W., Hilgen, F.J., Raffi, I., Sierro, F.J., Wilson, D.S., 1999. Chronology, causes and progression of the Messinian salinity crisis. *Nature* 400, 652–655. <https://doi.org/10.1038/23231>.
- Hilgen, F., Kuiper, K., Krijgsman, W., Snel, E., van der Laan, E., 2007. Astronomical tuning as the basis for high resolution chronostratigraphy: the intricate history of the Messinian Salinity Crisis. *Stratigraphy* 4, 231–238.
- Hüneke, H., Stow, D.A.V., 2008. Identification of ancient contourites: Problems and palaeoceanographic significance. In: *Rebecco, M., Camerlenghi, A. (Eds.), Contourites. Developments in Sedimentology, vol. 60. Elsevier, Amsterdam, pp. 323–344.*
- Iribarren, L., Vergés, J., Camurri, F., Fulla, J., Fernández, M., 2007. The structure of the Atlantic–Mediterranean transition zone from the Alboran Sea to the Horseshoe Abyssal Plain (Iberia–Africa plate boundary). *Mar. Geol.* 243, 97–119. <https://doi.org/10.1016/j.margeo.2007.05.011>.
- Ivanovic, R.F., Flecker, R., Gutjahr, M., Valdesa, P.J., 2013. First Nd isotope record of Mediterranean–Atlantic water exchange through the Moroccan Rifian Corridor during the Messinian Salinity Crisis. *Earth Planetary Science Letters* 368, 163–174. <https://doi.org/10.1016/j.epsl.2013.03.010>.
- Krijgsman, W., Capella, W., Simon, D., Hilgen, F.J., Kouwenhoven, T.J., Meijer, P.Th., Sierro, F.J., Tulbure, M.A., van den Berg, B.C.J., van der Schee, M., Flecker, R., 2018. The Gibraltar Corridor: Watergate of the Messinian Salinity Crisis. *Mar. Geol.* 403, 238–246. <https://doi.org/10.1016/j.margeo.2018.06.008>.
- Levy, R.G., Tillay, R., 1962–2017. Maroc Septentrional (Chaîne du Rif), partie B. Livret-Guide des excursions A31 et C31. *Congres Geologique International, XIX session, Alger*. Pp. 8–65. In: *Capella, W., Matenco, L., Dmitrieva, E., Roest, W.M., Hessels, S., Hssain, M., Krijgsman, W. (Eds.), Thick-skinned Tectonics Closing the Rifian Corridor: Tectonophysics, 710, pp. 249–265. https://doi.org/10.1016/j.tecto.2016.09.028.*

- Liu, S., Hernández-Molina, F.J., Ercilla, G., Van Rooij, D., 2020. Sedimentary evolution of the Le Danois contourite drift systems (southern Bay of Biscay, NE Atlantic): a reconstruction of the Atlantic Mediterranean Water circulation since the Pliocene. *Mar. Geol.* 427, 106217. <https://doi.org/10.1016/j.margeo.2020.106217>.
- Llave, E., Hernández-Molina, F.J., Somoza, L., Díaz del Río, V., Stow, D.A.V., Maestro, A., Alveirinho Dias, J.M., 2001. Seismic stacking pattern of the Faro-Albufera contourite system (Gulf of Cadiz): a Quaternary record of paleoceanographic and tectonic influences. *Mar. Geophys. Res.* 22, 475–496. <https://doi.org/10.1023/A:1016355801344>.
- Llave, E., Schönfeld, J., Hernández-Molina, F.J., Mulder, T., Somoza, L., Del Río, V.D., Sánchez-Almazo, I., 2006. High-resolution stratigraphy of the Mediterranean outflow contourite system in the Gulf of Cadiz during the late Pleistocene: the impact of Heinrich events. *Mar. Geol.* 227, 241–262. <https://doi.org/10.1016/j.margeo.2005.11.015>.
- Llave, E., Hernández-Molina, F.J., Somoza, L., Stow, D.A.V., Díaz del Río, V., 2007. Quaternary evolution of the contourite depositional system in the Gulf of Cadiz. In: Viana, A.R., Rebesco, M. (Eds.), *Economic and Palaeoceanographic significance of Contourite Deposits*. Geological Society London Special Publication 276, 49–79. <https://doi.org/10.1144/GSL.SP.2007.276.01.03>.
- Llave, E., Matias, H., Hernández-Molina, F.J., Ercilla, G., Stow, D.A.V., Medialdea, T., 2011. Pliocene–Quaternary contourites along the northern gulf of Cadiz margin: sedimentary stacking pattern and regional distribution. *Geo-Mar. Lett.* 31, 377–390. <https://doi.org/10.1007/s00367-011-0241-3>.
- Llave, E., Hernández-Molina, F.J., García, M., Ercilla, G., Roque, C., Juan, C., Mena, A., Preu, B., Van Rooij, D., Rebesco, M., Brackenridge, R., Jané, G., Gómez-Ballesteros, M., Stow, D., 2019. Contourites along the Iberian continental margins: conceptual and economic implications. *Geological Society London Special Publications* 476, 403–436. <https://doi.org/10.1144/SP476-2017-46>.
- Lopes, F.C., Cunha, P.P., Le Gall, B., 2006. Cenozoic seismic stratigraphy and tectonic evolution of the Algarve margin (offshore Portugal, southwestern Iberian Peninsula). *Mar. Geol.* 231, 1–36. <https://doi.org/10.1016/j.margeo.2006.05.007>.
- Louarn, E., Morin, P., 2011. Antarctic intermediate water influence on Mediterranean Sea water outflow. *Deep-Sea Research I Oceanography Research Papers* 58, 932–942. <https://doi.org/10.1016/j.dsr.2011.05.009>.
- Maestro, A., Somoza, L., Medialdea, T., Talbot, C.J., Lowrie, A., Vázquez, J.T., Díaz-del-Río, V., 2003. Large-scale slope failure involving Triassic and Middle Miocene salt and shale in the Gulf of Cádiz (Atlantic Iberian margin). *Terra Nova* 15, 380–391. <https://doi.org/10.1046/j.1365-3121.2003.00513.x>.
- Maldonado, A., Somoza, L., Pallarés, L., 1999. The Betic orogen and the Iberian-African boundary in the Gulf of Cádiz: geological evolution (Central North Atlantic). *Mar. Geol.* 155, 9–43. [https://doi.org/10.1016/S0025-3227\(98\)00139-X](https://doi.org/10.1016/S0025-3227(98)00139-X).
- Manzi, V., Gennari, R., Lugli, S., Persico, D., Reghizzi, M., Roveri, M., Schreiber, B.C., Calvo, R., Gavioli, I., Gvirtzman, Z., 2018. The onset of the Messinian salinity crisis in the deep Eastern Mediterranean basin. *Terra Nova* 30, 189–198. <https://doi.org/10.1111/ter.12325>.
- Martín, J.M., Braga, J.C., Aguirre, J., Puga-Bernabéu, Á., 2009. History and evolution of the North-Betic Strait (Prebetic Zone, Betic Cordillera): a narrow, early Tortonian, tidal-dominated, Atlantic-Mediterranean marine passage. *Sediment. Geol.* 216, 80–90. <https://doi.org/10.1016/j.sedgeo.2009.01.005>.
- Medialdea, T., Vegas, R., Somoza, L., Vázquez, J.T., Maldonado, A., Díaz-del-Río, V., Maestro, A., Córdoba, D., Fernández-Puga, M.C., 2004. Structure and evolution of the “Olistostrome” complex of the Gibraltar Arc in the Gulf of Cádiz (eastern Central Atlantic): evidence from two long seismic cross-sections. *Mar. Geol.* 209, 173–198. <https://doi.org/10.1016/j.margeo.2004.05.029>.
- Medialdea, T., Somoza, L., Pinheiro, L.M., Fernández-Puga, M.C., Vázquez, J.T., León, R., Ivanov, M.K., Magalhaes, V., Díaz-del-Río, V., Vegas, R., 2009. Tectonics and mud volcano development in the Gulf of Cádiz. *Mar. Geol.* 261, 48–63. <https://doi.org/10.1016/j.margeo.2008.10.007>.
- Menard, H.W., 1955. Deformation of the northeastern Pacific basin and the west coast of North America. *Geol. Soc. Am. Bull.* 66, 1149–1198. [https://doi.org/10.1130/0016-7606\(1955\)66\[1149:DOTNPB\]2.0.CO;2](https://doi.org/10.1130/0016-7606(1955)66[1149:DOTNPB]2.0.CO;2).
- Mencaroni, D., Urgeles, R., Ford, J., Llopert, J., Sánchez Serra, C., Calahorrano, A., Brito, P., Lo Iacono, C., Bartolomé, R., Gràcia, E., Rebesco, M., Camerlenghi, A., Bellwald, B., 2020. How deep does sand deposits in the Alentejo basin (Gulf of Cadiz) reach? Evaluating slope stability from bottom-current activities through time. In: EGU General Assembly 2020, 4–8 May 2020, pp. EGU2020–18904. <https://doi.org/10.5194/egusphere-egu2020-18904>.
- Mestdagh, T., Lobo, F.J., Llave, E., Hernández-Molina, F.J., Van Rooij, D., 2019. Review of the late Quaternary stratigraphy of the northern Gulf of Cadiz continental margin: New insights into controlling factors and global implications. *Earth Science Reviews* 178, 102944. <https://doi.org/10.1016/j.earscirev.2019.102944>.
- Mestdagh, T., Lobo, F.J., Llave, E., Hernández-Molina, F.J., García Ledesma, A., Puga-Bernabéu, Á., Fernández-Salas, L.-M., Rooij, D.V., 2020. Late Quaternary multi-genetic processes and products on the northern Gulf of Cadiz upper continental slope (SW Iberian Peninsula). *Mar. Geol.* 427, 106214. <https://doi.org/10.1016/j.margeo.2020.106214>.
- Miramontes, E., Eggenhuisen, J.T., Jacinto, R.S., Poneti, G., Pohl, F., Normandeau, A., Campbell, D.C., Hernández-Molina, F.J., 2020. Channel-levee evolution in combined contour current-turbidity current flows from flume-tank experiments. *Geology* 48, 353–357. <https://doi.org/10.1130/G47111.1>.
- Mitchum Jr., R.M., Vail, P.R., Sangree, J.B., 1977. Seismic stratigraphy and global changes of sea level; part 6, Stratigraphic interpretation of seismic reflection patterns in depositional sequences. In: Payton, C.E. (Ed.), *Seismic stratigraphy – applications to hydrocarbon exploration*. American Association of Petroleum Geologists (AAPG) Memoir 26, 117–133.
- Mulder, T., Faugères, J.-C., Gonthier, E., Rebesco, M., Camerlenghi, A., 2008. Mixed turbidite-contourite systems. In: Rebesco, M., Camerlenghi, A. (Eds.), *Contourites. Developments in Sedimentology*, vol. 60. Elsevier, Amsterdam, pp. 435–456. [https://doi.org/10.1016/S0070-4571\(08\)10021-8](https://doi.org/10.1016/S0070-4571(08)10021-8).
- Ng, Z.L., Hernández-Molina, F.J., Duarte, D., Sierro, F.J., Ledesma, S., Rogerson, M., Llave, E., Roque, C., Manar, M.A., 2021. Latest Miocene restriction of the Mediterranean Outflow Water: a perspective from the Gulf of Cádiz. *Geo-Marine Letters* 41, 23. <https://doi.org/10.1007/s00367-021-00693-9>.
- Nielsen, T., Knutz, P.C., Kuijpers, A., 2008. Seismic Expression of Contourite Depositional Systems. In: Rebesco, M., Camerlenghi, A. (Eds.), *Contourites. Developments in Sedimentology*, vol. 60. Elsevier, Amsterdam, pp. 301–321.
- O'Neill-Baringer, M., Price, J.F., 1997. Mixing and spreading of the Mediterranean outflow. *J. Phys. Oceanogr.* 27, 1654–1677. [https://doi.org/10.1175/1520-0485\(1997\)027<1654:MASOTM>2.0.CO;2](https://doi.org/10.1175/1520-0485(1997)027<1654:MASOTM>2.0.CO;2).
- Pellegrini, C., Maselli, V., Trincardi, F., 2016. Pliocene–Quaternary contourite depositional system along the south-western Adriatic margin: changes in sedimentary stacking pattern and associated bottom currents. *Geo-Mar. Lett.* 36, 67–79. <https://doi.org/10.1007/s00367-015-0424-4>.
- Pereira, R., Alves, T.M., 2013. Crustal deformation and submarine canyon incision in a Meso-Cenozoic first-order transfer zone (SW Iberia, North Atlantic Ocean). *Tectonophysics* 601, 148–162. <https://doi.org/10.1016/j.tecto.2013.05.007>.
- Pereira, R., Alves, T.M., Cartwright, J., 2011. Post-rift compression on the SW Iberian margin (eastern North Atlantic): a case for prolonged inversion in the ocean-continent transition zone. *J. Geol. Soc.* 168, 1249–1263. <https://doi.org/10.1144/0016-76492010-151>.
- Pereira, R., Alves, T.M., Mata, J., 2016. Alternating crustal architecture in West Iberia: a review of its significance in the context of NE Atlantic rifting. *J. Geol. Soc.* 174, 522–540. <https://doi.org/10.1144/jgs2016-050>.
- Pérez-Asensio, J.N., Aguirre, J., Schmiedl, G., Civis, J., 2012. Impact of restriction of the Atlantic-Mediterranean gateway on the Mediterranean Outflow Water and eastern Atlantic circulation during the Messinian. *Paleoceanography* 27, PA3222. <https://doi.org/10.1029/2012PA002309>.
- Posamentier, H.W., Erskine, R.D., 1991. Seismic Expression and Recognition Criteria of Ancient Submarine fans. In: Weimer, P., Link, M.H. (Eds.), *Seismic Facies and Sedimentary Processes of Submarine Fans and Turbidite Systems*. Frontiers in Sedimentary Geology. Springer, New York, pp. 197–222. https://doi.org/10.1007/978-1-4684-8276-8_10.
- Ramos, A., Fernández, O., Muñoz, J.A., Terrinha, P., 2017. Impact of basin structure and evaporite distribution on salt tectonics in the Algarve Basin, Southwest Iberian margin. *Mar. Pet. Geol.* 88, 961–984. <https://doi.org/10.1016/j.margeo.2017.09.028>.
- Rebesco, M., Hernández-Molina, F.J., Van Rooij, D., Wählin, A., 2014. Contourites and associated sediments controlled by deep-water circulation processes: State-of-the-art and future considerations. *Mar. Geol.* 352, 111–154. <https://doi.org/10.1016/j.margeo.2014.03.011>.
- Reed, D.L., Meyer, A.W., Silver, E.A., Prasetyo, H., 1987. Contourite sedimentation in an intracratonic forearc system: eastern Sunda Arc, Indonesia. *Mar. Geol.* 76, 223–241. [https://doi.org/10.1016/0025-3227\(87\)90031-4](https://doi.org/10.1016/0025-3227(87)90031-4).
- Rodrigues, S., Roque, C., Hernández-Molina, F.J., Llave, E., Terrinha, P., 2020. The Sines Contourite Depositional System along the SW Portuguese margin: onset, evolution and conceptual implications. *Mar. Geol.* 106357. <https://doi.org/10.1016/j.margeo.2020.106357>.
- Rodrigues, S., Hernández-Molina, F.J., Kirby, A., 2021. A late cretaceous mixed (turbidite-contourite) system along the Argentine margin: Paleoenvironmental and conceptual implications. *Mar. Pet. Geol.* 104768. <https://doi.org/10.1016/j.margeo.2020.104768>.
- Rogerson, M., Rohling, E.J., Weaver, P.P.E., 2006. Promotion of meridional overturning by Mediterranean derived salt during the last deglaciation. *Paleoceanography* 21, PA4101. <https://doi.org/10.1029/2006PA001306>.
- Rogerson, M., Rohling, E.J., Bigg, G.R., Ramirez, J., 2012. Palaeoceanography of the Atlantic-Mediterranean Exchange: Overview and first quantitative assessment of climatic forcing. *Rev. Geophys.* 50, RG2003. <https://doi.org/10.1029/2011RG000376>.
- Roque, C., Duarte, H., Terrinha, P., Valadares, V., Noiva, J., Cachão, M., Ferreira, J., Legoinha, P., Zitellini, N., 2012. Pliocene and Quaternary depositional model of the Algarve margin contourite drifts (Gulf of Cadiz, SW Iberia): seismic architecture, tectonic control and paleoceanographic insights. *Mar. Geol.* 303–306, 42–62. <https://doi.org/10.1016/j.margeo.2011.11.001>.
- Sánchez-Leal, R.F., Bellanco, M.J., Fernández-Salas, L.M., García-Lafuente, J., Gasser-Rubin, M., González-Pola, C., Hernández-Molina, F.J., Pelegrí, J.L., Peliz, A., Relvas, P., Roque, D., Ruiz-Villarreal, M., Sammartino, S., Sánchez-Garrido, J.C., 2017. The Mediterranean Overflow in the Gulf of Cadiz: a rugged journey. *Science Advances* 3, eaao0609. <https://doi.org/10.1126/sciadv.aao0609>.
- Serra, C.S., Martínez-Loriente, S., Gràcia, E., Urgeles, R., Vizcaino, A., Perea, H., Bartolome, R., Pallás, R., Lo Iacono, C., Díez, S., Dañobeitia, J., Terrinha, P., Zitellini, N., 2020. Tectonic evolution, geomorphology and influence of bottom currents along a large submarine canyon system: the São Vicente Canyon (SW Iberian margin). *Mar. Geol.* 426, 106219. <https://doi.org/10.1016/j.margeo.2020.106219>.
- Shanmugam, G., 2008. Deep-water bottom currents and their deposits. In: Rebesco, M., Camerlenghi, A. (Eds.), *Contourites. Developments in Sedimentology*, vol. 60. Elsevier, Amsterdam, pp. 59–81.
- Sierro, F.J., Hodell, D.A., Andersen, N., Azibeiro, L.A., Jimenez-Espejo, F.J., Bahr, A., Flores, J.A., Ausin, B., Rogerson, M., Lozano-Luz, R., Lebreiro, S.M., Hernández-Molina, F.J., 2020. Mediterranean overflow over the last 250 kyr: Freshwater forcing

- from the tropics to the ice sheets. *Paleoceanography and Paleoclimatology* 35. <https://doi.org/10.1029/2020PA003931> e2020PA003931.
- Srivastava, S.P., Schouten, H., Roest, W.R., Klitgord, K.D., Kovacs, L.C., Verhoef, J., Macnab, R., 1990. Iberian plate kinematics: a jumping plate boundary between Eurasia and Africa. *Nature* 344, 756–759. <https://doi.org/10.1038/344756a0>.
- Stow, D.A.V., Smillie, Z., 2020. Distinguishing between Deep-Water Sediment Facies: Turbidites, Contourites and Hemipelagites. *Geosciences* 10, 68. <https://doi.org/10.3390/geosciences10020068>.
- Stow, D.A.V., Hernández-Molina, F.J., Alvarez Zarikian, C.A., the Expedition 339 Scientists, 2013. Proceedings IODP, 339. Integrated Ocean Drilling Program Management International, Tokyo. <https://doi.org/10.2204/iodp.proc.339.2013>.
- Teixeira, M., Terrinha, P., Roque, C., Rosa, M., Ercilla, G., Casas, D., 2019. Interaction of alongslope and downslope processes in the Alentejo margin (SW Iberia) – Implications on slope stability. *Mar. Geol.* 410, 88–108. <https://doi.org/10.1016/j.margeo.2018.12.011>.
- Terrinha, P., Matias, L., Vicente, J., Duarte, J., Luís, J., Pinheiro, L., Lourenço, N., Diez, S., Rosas, F., Magalhães, V., Valadares, V., Zitellini, N., Roque, C., Mendes Víctor, L., MATESPRO Team, 2009. Strain partitioning and morphotectonics at the Iberia-Africa plate boundary from multibeam and seismic reflection data. *Mar. Geol.* 267, 156–174. <https://doi.org/10.1016/j.margeo.2009.09.012>.
- Terrinha, P., Kullberg, J.C., Neres, M., Alves, T., Ramos, A., Ribeiro, C., Mata, J., Pinheiro, L., Afilhado, A., Matias, L., Luís, J., Muñoz, J.A., Fernández, Ó., 2019a. Rifting of the Southwest and West Iberia Continental Margins. In: Quesada, C., Oliveira, J.T. (Eds.), *The Geology of Iberia: A Geodynamic Approach*. Regional Geology Reviews. Springer, Cham, pp. 251–283. https://doi.org/10.1007/978-3-030-11295-0_6.
- Terrinha, P., Ramos, A., Neres, M., Valadares, V., Duarte, J., Martínez-Loriente, S., Silva, S., Mata, J., Kullberg, J.C., Casas-Sainz, A., Matias, L., Fernández, Ó., Muñoz, J.A., Ribeiro, C., Font, E., Neves, C., Roque, C., Rosas, F., Pinheiro, L., Bartolomé, R., Sallarès, V., Magalhães, V., Medialdea, T., Somoza, L., Gràcia, E., Hensen, C., Gutscher, M.-A., Ribeiro, A., Zitellini, N., 2019b. The Alpine Orogeny in the West and Southwest Iberia margins. In: Quesada, C., Oliveira, J. (Eds.), *The Geology of Iberia: A Geodynamic Approach*. Regional Geology Reviews. Springer, Cham, pp. 487–505. https://doi.org/10.1007/978-3-030-11295-0_11.
- Torelli, L., Sartori, R., Zitellini, N., 1997. The giant chaotic body in the Atlantic Ocean off Gibraltar: new results from a deep seismic reflection survey. *Mar. Pet. Geol.* 14, 125–134. [https://doi.org/10.1016/S0264-8172\(96\)00060-8](https://doi.org/10.1016/S0264-8172(96)00060-8).
- Tortella, D., Torne, M., Pérez-Estáun, A., 1997. Geodynamic Evolution of the Eastern Segment of the Azores-Gibraltar Zone: the Gorringe Bank and the Gulf of Cadiz Region. *Mar. Geophys. Res.* 19, 211–230. <https://doi.org/10.1023/A:1004258510797>.
- van der Laan, E., Hilgen, F.J., Lourens, L.J., de Kaenel, E., Gabori, S., Iaccarino, S., 2012. Astronomical forcing of Northwest African climate and glacial history during the late Messinian (6.5–5.5 Ma). *Palaeogeogr. Palaeoclimatol. Palaeoecol.* 313, 107–126. <https://doi.org/10.1016/j.palaeo.2011.10.013>.
- van der Schee, M., Sierro, F., Jimenez-Espejo, F., Hernández-Molina, F., Flecker, R., Flores, J., Acton, G., Gutjahr, M., Grunert, P., García-Gallardo, A., Andersen, N., 2016. Evidence of early bottom water current flow after the Messinian Salinity Crisis in the Gulf of Cádiz. *Mar. Geol.* 380, 315–329. <https://doi.org/10.1016/j.margeo.2016.04.005>.
- Vancraeynest, F., 2015. Contourite Depositional Systems in the El Arraiche Area, Moroccan Atlantic Margin. Master's dissertation. Universiteit Gent. https://lib.ugent.be/fulltxt/RUG01/002/213/957/RUG01-002213957_2015_0001_AC.pdf.
- Vandorpe, T., Van Rooij, D., de Haas, H., 2014. Stratigraphy and paleoceanography of a topography-controlled contourite drift in the Pen Duick area, southern Gulf of Cádiz. *Mar. Geol.* 349, 136–151. <https://doi.org/10.1016/j.margeo.2014.01.007>.
- Verdicchio, G., Trincardi, F., 2008. Shallow-water Contourites. In: Rebesco, M., Camerlenghi, A. (Eds.), *Contourites*. Developments in Sedimentology, vol. 60. Elsevier, Amsterdam, pp. 409–433.
- Vergés, J., Fernández, M., 2012. Tethys–Atlantic Interaction along the Iberia–Africa Plate Boundary: The Betic–Rif Orogenic System. *Tectonophysics* 579, 144–172. <https://doi.org/10.1016/j.tecto.2012.08.032>.
- Zitellini, N., Rovere, M., Terrinha, P., Chierici, F., Matias, L., Team, Bigsets, 2004. Neogene through Quaternary Tectonic Reactivation of SW Iberian Passive margin. *Pure Appl. Geophys.* 161, 565–587. <https://doi.org/10.1007/s00024-003-2463-4>.